bioRxiv preprint doi: https://doi.org/10.1101/2022.06.02.494553; this version posted June 3, 2022. The copyright holder for this preprint (which was not certified by peer review) is the author/funder, who has granted bioRxiv a license to display the preprint in perpetuity. It is made available under aCC-BY-NC-ND 4.0 International license.

Population Sequencing Reveals *Rht-D1b* Contributing the Bigger Seedling Root to Modern Wheat Cultivars

Xiaoming Wang[1,3], Peng Zhao[1,3], Xiaolong Guo[1,3], Zihui, Liu[1], Xiuyun Ma[1], Yuqian Zhao[1], Xiangjun Lai[1], Liuying Huang[1], Wanying Wang[1], Dejun Han[1], Zhensheng Kang[2,*], Shengbao Xu[1,*]

[1]State Key Laboratory of Crop Stress Biology for Arid Areas, College of Agronomy, Northwest A&F University, Yangling, Shaanxi, 712100, China.

[2]State Key Laboratory of Crop Stress Biology for Arid Areas and College of Plant Protection, Northwest A&F University, Yangling, Shaanxi 712100, China.

[3]These authors contributed equally: Xiaoming Wang, Peng Zhao and Xiaolong Guo.

* Correspondence: xushb@nwsuaf.edu.cn and kangzs@nwsuaf.edu.cn

Short Title: *Rht-D1b* shapes the modern wheat root

One-sentence Summary: The suppressed GA signaling by *Rht-D1b* promotes root cell width, conferring a bigger root system and higher root-shoot ratio to modern wheat cultivars.

The author responsible for the distribution of materials integral to the findings presented in this article in accordance with the policy described in the Instructions for Authors (www.plantcell.org) is: Shengbao Xu (xushb@nwsuaf.edu.cn).

ABSTRACT

The crop root system is pivotal for water and nutrient uptake and environmental stress adaptations. Wheat, as the major calorie provision for the world's population, successfully increases its yield for world population expansion with modern breeding selection. However, the root adaptation in modern wheat cultivars still remain unknown. Here we present the root transcriptomes of 351 wheat accession, which

bioRxiv preprint doi: https://doi.org/10.1101/2022.06.02.494553; this version posted June 3, 2022. The copyright holder for this preprint (which was not certified by peer review) is the author/funder, who has granted bioRxiv a license to display the preprint in perpetuity. It is made available under aCC-BY-NC-ND 4.0 International license.

showed a distinct transcriptomic profile between landraces (LA) and modern cultivars (MC), suggesting a significant change of MC in environmental adaptation and root development. The MC seedlings showed a significantly bigger root system, which is mainly contributed by the well-known green revolution allele *Rht-D1b*. The suppressed GA signaling by *Rht-D1b* inhibits the cell length in above-ground tissue for a dwarf structure, but increases the cell width in the root meristem, resulting in bigger root diameter and a bigger root volume. This distinct regulation between above- and under-ground contribute a significantly larger root-shoot ratio to modern wheat cultivars. Our data provide new insights for the successful adoption of *Rht-D1b* and *Rht-B1b* in green revolution, and the application of *Rht-D1b* and *Rht-B1b* in future wheat breeding and production.

bioRxiv preprint doi: https://doi.org/10.1101/2022.06.02.494553; this version posted June 3, 2022. The copyright holder for this preprint (which was not certified by peer review) is the author/funder, who has granted bioRxiv a license to display the preprint in perpetuity. It is made available under aCC-BY-NC-ND 4.0 International license.

INTRODUCTION

Root system is fundamental for crop water and nutrient uptakes (Den Herder et al., 2010; van der Bom et al., 2020), also critical for abiotic stress adaptation (Lynch, 1995; Khan et al., 2016; Hu et al., 2019; Calleja-Cabrera et al., 2020; de Vries et al., 2020). The monocotyledonous wheat root system is composed of seminal roots and adventitious roots. The seminal root system develops initially and consists of the primary root and two pairs of seminal roots (Hou et al., 2019; Hendel et al., 2021). Seminal roots penetrate the soil earlier and deeper than the adventitious roots and usually remain active throughout the plant life cycle, and play a crucial role in absorbing water from deep soil layers (Watt et al., 2008). Although the root length and more seminar roots are important for wheat survival under water limitation (Golan et al., 2018; Bacher et al., 2021), there is a trade-off between longer roots or more roots (van der Bom et al., 2020). Actually, the root structure has to match the surrounding environments to maximise the nutrients and water intake from the soil. It is difficult to define an ideal root structure for a plant (van der Bom et al., 2020).

Modern bread wheat (*Triticum aestivum* L.) is hexaploidy comprising A, B and D subgenomes (IWGSC, 2018; Zhou et al., 2020). Wheat root had experienced a suite of complex genetic, morphological and physiological function modifications during wheat evolution and domestication (Abbo et al., 2014; Golan et al., 2018), including drought tolerance improvement (Golan et al., 2018; Bacher et al., 2021). Over the past century, wheat grain yield has been remarkably improved with the breeding activities targeting high-yield (Godfray et al., 2010; van de Wouw et al., 2010; Snowdon et al., 2020). This breeding selection has largely reshaped the wheat genome and made the modern cultivars (MC) different from the landrace (LA) (Hu et al., 2019; Hao et al., 2020; Zhou et al., 2020). Significantly, the Green Revolution of the 1960s, by introducing semi-dwarfing genes into rice and wheat, dramatically increased cereal grain yields that were associated with improved lodging resistance and the resulting ability to tolerate higher levels of inorganic nitrogen-based fertilizer (Pearce et al.,

bioRxiv preprint doi: https://doi.org/10.1101/2022.06.02.494553; this version posted June 3, 2022. The copyright holder for this preprint (which was not certified by peer review) is the author/funder, who has granted bioRxiv a license to display the preprint in perpetuity. It is made available under aCC-BY-NC-ND 4.0 International license.

2011; Van De Velde et al., 2021). However, how the modern wheat cultivars adjust root development to fit the current cultivation conditions and yield production remains largely unknown.

In hexaploid wheat, dwarfing has been achieved mainly through the introduction of the *Rht* (Reduced Height) alleles *Rht-B1b* and *Rht-D1b* (previously named *Rht1* and *Rht2*), which introduce premature stop codons in the N-terminal coding region of DELLA proteins and confer lower sensitivity to GA (Wu et al., 2011; Liu et al., 2021). After six decades of practice, approximately 70% of cultivars in a worldwide wheat panel released in the 21st century carry one of these two alleles (Wurschum et al., 2017). They significantly altered plant structure related traits (Lanning et al., 2012; Sherman et al., 2014), but the root changes with the dwarf alleles' introduction remain largely unclear.

With the increase in sequencing accuracy, large-scale population transcriptome sequencing is becoming an efficient tool for SNP identification (Fu et al., 2013; Zhang et al., 2017). The transcriptome data also provide a link between the traits and the SNP variations that cannot be readily captured at the sequence level (Azodi et al., 2020), thus providing an important bridge from DNA to phenotypes and critical clues for the investigation of underlying mechanisms of functional variations. However, current population genetics is challenged by the interference from population structure and membership kinship, which results in different outputs with the varied population composition (Fauman, 2020). Therefore, many new approaches and concepts were developed to support current population genetics, including the differentially expressed genes in population and random population combination analysis (Bulik-Sullivan et al., 2015; Chen et al., 2021; Li et al., 2022).

Here, we performed transcriptome sequencing and phenotyping on seedling root for a natural bread wheat population, including 87 landraces and 264 historical modern cultivars, revealing that the modern wheat breeding selection reshaped the root transcriptomes and root development. Our results demonstrated that *Rht-D1b* is

bioRxiv preprint doi: https://doi.org/10.1101/2022.06.02.494553; this version posted June 3, 2022. The copyright holder for this preprint (which was not certified by peer review) is the author/funder, who has granted bioRxiv a license to display the preprint in perpetuity. It is made available under aCC-BY-NC-ND 4.0 International license.

the major allele contributing a bigger root system to modern wheat cultivars. The population transcriptome analysis showed that *Rht-D1b* regulates a broad of genes involved in wheat root development, increases increased the root cell width and root diameter, thereby significantly enhances the root-shoot ratio of modern wheat, which provides new insights for *Rht-D1b* application in futural wheat breeding practice.

RESULTS

Root transcriptome sequencing of natural wheat population

A total of 385 worldwide bread wheat accessions (Table S1) were collected and sequenced the transcriptome with the seedling roots, producing 15.08 billion high-quality reads and identifying 1,225,246 SNPs with an average density of 8 SNPs per gene or approximate one SNP per 944 bp (Fig. 1A), providing a more detailed variation landscape for the wheat genome. About half of SNPs (48%) are located in the CDS (coding sequence) regions (Fig. 1B), demonstrating a feature of the transcriptome derived SNPs.

The expression evidence of 107,651 genes was identified in this population, including 39,277 wheat low confidence (LC) genes, extending the number of reliable wheat genes to the current wheat genome. The expression levels of genes in the population ranged from 0.5 to 21144.5 TPM (transcript per million). The highly expressed genes are enriched in the category of “response to water deprivation” and “water transport” (Fig. 1C and Table S2), highlighting the root function as the water uptake organ. Interestingly, the categories of “response to water deprivation” and “water transport” are also enriched in the highly varied expression genes in this natural population (Fig. 1D and Table S3), indicating water intake process is highly varied among wheat accessions which present a great potential to improve based on the current wheat germplasms.

Modern wheat breeding substantially reshaped the root transcriptome and root development

bioRxiv preprint doi: https://doi.org/10.1101/2022.06.02.494553; this version posted June 3, 2022. The copyright holder for this preprint (which was not certified by peer review) is the author/funder, who has granted bioRxiv a license to display the preprint in perpetuity. It is made available under aCC-BY-NC-ND 4.0 International license.

Based on the phylogenetic analysis with clear definition varieties, ancestry coefficient estimation and the pedigree documentation, 264 modern cultivars (MC) and 87 landraces (LA) were determined (Fig. 2A and 2B). An average of 7,185 differentially expressed genes (DEGs) between LA and MC groups could be identified (FDR adjusted P-value < 0.01; Table S4) with Wilcoxon rank-sum test (Li et al., 2022), followed by cross-validation based on 100 random permutations to exclude the population structure interference (Fig. 2C). In contrast, there were only 0.2% of the whole population based 100,000 permutations in which DEG was detected, and only 16 out of the 100,000 tests showed a similar DEG number (7,185) with that between MC and LA (Fig. 2C) suggesting that MC had accumulated a vast difference in root transcriptome during the modern breeding selection.

To improve the reliability, the DEGs that were detected more than ten times in the 100 permutations (Fig. 2C) were used for enrichment analysis. GO analysis reveals that modern wheat cultivars significantly changed in environmental stress response, development, metabolic processes and signaling transductions (Fig. 2D and Table S5).

There are 161 genes identified as the DEGs between MC and LA, which pass all 100 random permutations (Table S6). Of which, the homologs of 12 genes in other plants were identified as the key genes involved in root development, including *AtACR4* (De Smet et al., 2008; Yue et al., 2016), *AtRCD1* (Teotia and Lamb, 2011), *AtARR10* (Yokoyama et al., 2007; Zubo et al., 2017), two *AtGSTU17* (Chen et al., 2012), *AtACT7* (Gilliland et al., 2003), *AtNRP2* (Wu et al., 2022), *AtHB-15* (Ohashi-Ito and Fukuda, 2003), three *AtKNAT3* (Truernit et al., 2006) and *AtEXPB2* (Wu et al., 2001), indicating that the root development may be altered with modern wheat breeding.

To clarify root developmental alterations of MC, the root phenotypes of 14 days after germination (DAGs) seedlings were investigated (Fig. 2E). We found the root

bioRxiv preprint doi: https://doi.org/10.1101/2022.06.02.494553; this version posted June 3, 2022. The copyright holder for this preprint (which was not certified by peer review) is the author/funder, who has granted bioRxiv a license to display the preprint in perpetuity. It is made available under aCC-BY-NC-ND 4.0 International license.

surface and volume were significantly increased in the MC group, albeit the primary root and total root length showed no significant difference. The root number and root diameter are also significantly increased in the MC group, which may be responsible for the bigger root system of MC.

The *Rht-D1b* contributes the major effect in increasing seedling root volume of modern wheat cultivars

GWAS analysis showed a QTL on 4D that was significantly associated with the root surface and volume, which contained the well-known *Rht-D1*, contributing to 14-23% variation of these traits in the population (Fig. 3A, Supplemental Table S7). The Transcriptome Wide Association Study (TWAS) showed that the *Rht-D1* ranked first in assigning as the casual gene, and its transcriptional level was positively correlated with these two traits (Fig. 3B, Supplemental Table S8). In population transcriptomic data, the *Rht-D1* has a significantly higher transcriptional level in *Rht-D1b* genotypes than that in *Rht-D1a* genotypes (Fig. 3C), consistent with the larger root surface and volume in *Rht-D1b* genotypes.

Surprisingly, the root surface and volume in modern wheat showed no difference from that of LA if we removed the cultivars containing *Rht-D1b* (Fig. 3D). Meanwhile, the root surface and volume of the *Rht-D1b* genotypes were significantly higher than that of the *Rht-D1a* genotypes, supporting that the *Rht-D1b* is the major allele conferring the bigger root system to modern wheat. Besides, the total root length and root diameter were also significantly increased in *Rht-D1b* genotypes (Fig. 3D), supporting *Rht-D1b* also played a crucial role in modifying modern wheat root system in addition to dwarf the wheat structure.

To exclude the possibility that the bigger root system of the *Rht-D1b* was raised from the earlier germination, the seedling root development was systematically and continuously investigated (Fig. 3E). The results showed that the root length is significantly shorter in the *Rht-D1b* genotypes at 4 DAGs; then, it catches up with the

bioRxiv preprint doi: https://doi.org/10.1101/2022.06.02.494553; this version posted June 3, 2022. The copyright holder for this preprint (which was not certified by peer review) is the author/funder, who has granted bioRxiv a license to display the preprint in perpetuity. It is made available under aCC-BY-NC-ND 4.0 International license.

seedling development process. At seven DAGs, the *Rht-D1b* genotypes showed a significant increase in root diameter and volume than other genotypes. The total root length and root surface significantly increased until 14 DAGs (Fig. 3E). These observations suggest that the bigger root of *Rht-D1b* is from the faster growth after germination instead of the earlier germination.

The full CDS containing *Rht-D1b* allele driven by the *Rht-D1* promoter was introduced into wheat cv Fielder (*Rht-D1a* and *Rht-B1b* background), which confirmed its role in increasing total root length, root diameter, and a bigger root system (Fig. 3F), supporting that the *Rht-D1b* has a versatile role in regulating wheat root development.

The bigger root system of the *Rht-D1b* depends on the GA signaling

The *Rht* genes encode DELLA, which acts as the key negative regulator of the GA signaling, prompting us to investigate the role of GA in the regulation of *Rht-D1b* on root development. Eighteen accessions were randomly selected from the *Rht-D1b*, *Rht-B1b* and *Rht-B1aRht-D1*a (marked NO) groups, respectively, and treated by exogenous GA in the hydroponics system. We found that the root length of the *Rht-D1b* and the *Rht-B1b* were significantly longer than that in *NO* genotypes under normal conditions, while the leaf length showed the opposite trend. After the exogenous GA treatment, the above-ground growth was promoted, but the underground root growth was significantly inhibited in *NO* genotypes (Fig. 4A), highlighting the different effects of GA on above- and under-ground tissues. Both cultivars containing *Rht-B1b* and *Rht-D1b* showed lower sensitivity to exogenous GA treatment, although they displayed similar responsive trends with the *NO* in above- and under-ground tissues, suggesting a suppressed GA signaling by the *Rht-B1b* and *Rht-D1b* introduction. A parallel experiment in which wheat seedlings were cultivated in soil and were treated by spraying exogenous GA on leaves, which showed the increased leaf length under GA treatment, especially in the *NO* genotypes, but no

bioRxiv preprint doi: https://doi.org/10.1101/2022.06.02.494553; this version posted June 3, 2022. The copyright holder for this preprint (which was not certified by peer review) is the author/funder, who has granted bioRxiv a license to display the preprint in perpetuity. It is made available under aCC-BY-NC-ND 4.0 International license.

difference for root related traits (Fig. 4B), further supporting that GA signaling promoted the growth of above-ground tissue. Importantly, these observations suggested GA confers an opposite effect on above- and under-ground tissue growth and the bigger root system of the *Rht-D1b* is related to the GA signaling, as the typical semidwarf plant height conferred by the suppressed GA signaling (Rizza and Jones, 2019).

This analysis indicates that the *Rht-B1b* may also contribute to the modern wheat root trait by suppressing the GA signaling. However, there is no significant association between *Rht-B1b* and root related traits in our GWAS analysis, which prompted us to further compare the effects of *Rht-D1b* and *Rht-B1b* on root development using 92 *Rht-D1b*, 70 *Rht-B1b* and 188 *NO* genotypes in our population. The results showed that the *Rht-B1b* indeed had the same function in enhancing the root system as *Rht-D1b* (Fig. 4C). However, all its effects were weaker than *Rht-D1b*, and more dependent on genetic background as demonstrated the smaller chance in the permutations. We speculated that the missed *Rht-B1b* in the GWAS analysis might result from the mask of the stronger *Rht-D1b* effect, then divided into two groups by removing the cultivars containing *Rht-B1b* or *Rht-D1b*, respectively. We found the contribution of *Rht-D1b* significantly increased in the population without *Rht-B1b* genotypes, indicating that the *Rht-B1b* has an interfering effect on the *Rht-D1b* association. However, the *Rht-B1b* still could not be detected when we removed the *Rht-D1b* genotypes from the population (Fig. 4D, Table S9), further supporting the stronger effect of *Rht-D1b* in regulating modern wheat root development.

The cell size alteration underlying the regulation mechanism of *Rht-D1b*

To clarify the underlying mechanism of *Rht-D1b* in regulating root development, the DEGs derived from the introduction of *Rht-D1b* and *Rht-B1b* were identified by comparing the gene expressions between *Rht-D1b* and *Rht-B1* genotypes and *NO* genotypes, respectively (Fig. 5A). The enriched analysis demonstrates that the

bioRxiv preprint doi: https://doi.org/10.1101/2022.06.02.494553; this version posted June 3, 2022. The copyright holder for this preprint (which was not certified by peer review) is the author/funder, who has granted bioRxiv a license to display the preprint in perpetuity. It is made available under aCC-BY-NC-ND 4.0 International license.

introduction of *Rht-D1b* down-regulated the expression of genes related to "Protein targeting to vacuole", "Cell wall organization", "Cell wall modification", and "Regulation of root meristem growth" (Fig. 5B, Table S10), indicating that the morphology and development of root cells experienced a significant alteration with *Rht-D1b* introduction.

The root meristem was investigated in *Rht-D1b* transgenic lines, and the results showed that the meristem length and width of *Rht-D1b* were significantly increased (Fig. 5C). The cell width in the meristem zone is increased (Fig. 5C), which would be the reason for the larger meristem width. The cell number of longitudinal meristem is significantly increased while the average cell length keeps similar to that of wildtype. Considering that the half-length of cell width was used to define the meristem region, the increased dividing cell number and meristem length may also be derived from the increased cell width. Then, we investigated the cells in the mature root region and showed that both the cell length and the cell width increased, suggesting that the *Rht-D1b* has a key role in increasing the size of root cells.

Meanwhile, the cell size of above-ground tissues was also investigated. We found that the cells decrease in length but not the width, consistent with their well-known dwarf phenotype, further supporting the distinct regulation pattern of GA signaling between above- and under-ground tissues.

Rht-D1b showed a broader regulatory gene spectrum that was related to root development

To characterize the underlying mechanism of the stronger effect of *Rht-D1b* in regulating wheat root phenotypes, the DEGs between *Rht-D1b* and *NO* genotypes and *Rht-B1b* and *NO* genotypes were identified. The results showed that 3,407 and 464 DEGs were raised with the *Rht-D1b* and *Rht-B1b* introduction, respectively, and 195 DEGs were shared between these two comparisons (Fig. 6A), indicating that the *Rht-D1b* had a broader influence on the root transcriptome. On the other hand, the

bioRxiv preprint doi: https://doi.org/10.1101/2022.06.02.494553; this version posted June 3, 2022. The copyright holder for this preprint (which was not certified by peer review) is the author/funder, who has granted bioRxiv a license to display the preprint in perpetuity. It is made available under aCC-BY-NC-ND 4.0 International license.

Rht-D1b didn't confer a stronger regulatory effect on the transcriptions of the common DEGs (Fig. 6B), indicating the stronger phenotypes of *Rht-D1b* may not be from its stronger inhibitory effect on GA signaling.

The co-expression analysis showed that the co-expressed genes ($p < 10^{-10}$) with *Rht-D1* are more than that with *Rht-B1* in *NO* genotypes. The co-expressed genes with *Rht-D1* almost cover all the co-expressed genes of *Rht-B1b*, supporting *Rht-D1* has a bigger gene co-expression network. Further analysis showed that the *Rht-D1b* have 523 co-expressed genes out of the whole gene network of all three *Rhts* (Rht-A1, B1, and D1), while only 1 gene is co-expressed with *Rht-B1b* under this circumstance, further support that the *Rht-D1b* has a broader regulatory gene spectrum, compared to that of *Rht-B1b*.

There are several DEGs whose homologs were reported to be involved in cell proliferation and root development, including At*GIF3* (Lee et al., 2009) and *AtP23-2* (D'Alessandro et al., 2015), were specifically regulated by the *Rht-D1b* but not the *Rht-B1b* (Fig. 6D), further supporting the assumption that *Rht-B1b* and *Rht-D1b* had diverged functions in root development regulation. However, the specific mechanism still needs further investigation.

Interestingly, the two major wheat regions in China, the Yellow and Huai wheat production region (Y&H) and Yangtze River winter wheat production region (YR) (Fig. 6E), showed a distinct preference for these two alleles, that modern wheat cultivars in Y&H mainly selected the *Rht-D1b* while almost all of the YR cultivars selected *Rht-B1b*, which may be related the root traits of these two alleles.

The opposite GA responses between above- and under-ground contribute to a higher root-shoot ratio

The reversed effects of GA on above- and under-ground traits (Fig. 4A, 4B, 5C) suggested a role of *Rht-B1b* and *Rht-D1b* in regulating wheat root-shoot ratio. To confirm this hypothesis, the fresh weight of shoot and root at seven DAGs were

bioRxiv preprint doi: https://doi.org/10.1101/2022.06.02.494553; this version posted June 3, 2022. The copyright holder for this preprint (which was not certified by peer review) is the author/funder, who has granted bioRxiv a license to display the preprint in perpetuity. It is made available under aCC-BY-NC-ND 4.0 International license.

284 investigated. The results showed that the root-shoot ratio was significantly increased
285 in *Rht-D1b* and *Rht-B1b* genotypes (Fig. 7A). GWAS identified *Rht-D1b* as the
286 critical allele to increase the root-shoot ratio of modern wheat cultivars (Fig. 7B). The
287 *Rht-B1b* was also significantly associated with the higher root-shoot ratio when the
288 *Rht-D1b* genotypes were removed, suggesting a stronger effect of *Rht-D1b,* which
289 masked the effect of *Rht-B1b*. In turn, the contribution and reliability of the *Rht-D1b*
290 association in GWAS obviously increased when the *Rht-B1b* genotypes were removed,
291 indicating the interference from *Rht-B1b*. These results suggested that *Rht-D1b* and
292 *Rht-B1b* significantly increased the root-shoot ratio at the early developmental stage
293 and provided new insights for understanding the successful utilization of the green
294 revolution alleles.

295 Collectedly, our results showed that the introduction of *Rht-D1b* and *Rht-B1b* into
296 modern wheat suppressed the GA signaling, which conferred distinct GA responses
297 between above- and under-ground tissues, increased the cell width in root but
298 inhibited the cell length in above-ground tissues, conferred a bigger root system and a
299 higher root-shoot ratio (Figure 7C). The *Rht-D1b* confers a stronger effect in
300 enhancing wheat root system and root-shoot ratio, which significantly changed the
301 root related traits of current wheat cultivars.

302 **DISCUSSION**

303 In this study, the large-scale transcriptome sequencing provides a high-density
304 SNP marker for gene evaluation. Meanwhile, 39277 LC genes were identified in the
305 wheat root, providing transcriptional evidence for LC genes and extending the wheat
306 genome database. Based on the identified SNP and wheat root phenotyping, the
307 well-known green revolution allele *Rht-D1b* was identified as the major allele for
308 enhancing the root system in modern wheat cultivars.

309 Although the TWAS was applied in many plant population transcriptomes
310 (Kremling et al., 2019; Wainberg et al., 2019), the *Rht-D1b* identification with TWAS

bioRxiv preprint doi: https://doi.org/10.1101/2022.06.02.494553; this version posted June 3, 2022. The copyright holder for this preprint (which was not certified by peer review) is the author/funder, who has granted bioRxiv a license to display the preprint in perpetuity. It is made available under aCC-BY-NC-ND 4.0 International license.

was still unexpectedly in this study. This significant association maybe just resulted from the significantly changed expression of *Rht-D1* with the *Rht-D1b* introduction (Fig. 3D). The underlying correlation between the SNP and the higher expression of *Rht-D1b* requires further elucidation.

It has been suggested that targeting roots for crop improvement may be the solution to the second Green Revolution (Lynch, 2007; Den Herder et al., 2010). Although the increased root length or root number could increase the root system, the larger root diameter derived from the *Rht-B1b* and *Rht-D1b* introduction is the major reason to contributes to a bigger root volume in our study. This result enlightens a new direction for root improvement by enhancing root cell width and root diameter, which would bypass the competition between the longer root and more root number (van der Bom et al., 2020) to form a bigger root system.

The *Rht-D1b* contributed a larger seedling root to modern wheat and was preferentially adopted in the Y&H wheat production region. The drought and cold winter ecology conditions in Y&H may be the important reason for *Rht-D1b* adoption here. It will be an interesting and important question to clarify the connections between the bigger root system and its geographic adoption in China (Zhang et al., 2006; Gao et al., 2015), USA (Guedira et al., 2010) and Europe (Wurschum et al., 2015; Wurschum et al., 2018).

Although Gibberellins can enhance root cell elongation (Shani et al., 2013) and root meristem proliferation (Qin et al., 2022), the increase of cell width by *Rht-D1b* is actually responsible for the bigger root system. Similarly, the cell length reduction is the major mechanism for the dwarf phenotypes, suggesting the critical role of GA in controlling plant cell shape.

The diverged GA signaling responses between the above- and under-ground tissue were due to their distinct GA sensitivity (Tanimoto, 2012). The reduced GA production has little influence on root growth. In contrast, over-produced GA

bioRxiv preprint doi: https://doi.org/10.1101/2022.06.02.494553; this version posted June 3, 2022. The copyright holder for this preprint (which was not certified by peer review) is the author/funder, who has granted bioRxiv a license to display the preprint in perpetuity. It is made available under aCC-BY-NC-ND 4.0 International license.

significantly inhibits root growth (Qin et al., 2022), consistent with that the root is very sensitive to GA and reaches the saturated status with low concentration maintenance (Tanimoto, 2012). In this study, both *Rht-B1b* and *Rht-D1b* genotypes showed a decreased sensitivity for GA treatment, while still responding to the exogenous GA (Fig. 5A) to inhibit root growth, indicating that the suppressed GA signaling in *Rht-B1b* and *Rht-D1b* is a benefit for the root development. However, these data suggest the GA signaling seems contribute a negative effect on root growth in *NO* genotype wheat, which is contradict to the previous conclusion that the low GA concentration could promote root growth in most plant species (Tanimoto, 2012), thus, the underlying mechanism remains largely unknown.

In plants, the GA synthesis and transportation (Topham et al., 2017; Binenbaum et al., 2018) is a complex gene network. Moreover, the roles of GA in the plant are spatial (Topham et al., 2017) and temporal dependent (Qin et al., 2022), which challenges our understanding of the regulatory mechanisms of *Rht-B1b* and *Rht-D1b*. Here, the new finding that the distinct effect between above- and underground of GA, the functions in increasing root diameter and root-shoot ratio of *Rht-B1b* and *Rht-D1b*, and the diverged functions between *Rht-B1b* and *Rht-D1b* will benefit futural wheat breeding and cultivation practices, shedding new light on the regulatory mechanisms of GA in the plant.

Materials and Methods

Plant materials, root development trait measurement, and RNA sequencing

The seeds of 385 bread wheat accessions (Table S1) were sterilized with 2% NaClO and then grown on water-soaked filter papers in germination boxes under the conditions of 22 ℃/16 ℃ day/night (50% relative air humidity) and 16h light (2000 Lux) / 8h dark. Six biological replicates were carried out to obtain robust results. During growth, the sterilized water in germinating boxes was replaced regularly. For each accession, at least three root samples per biological replicate were collected at 14

bioRxiv preprint doi: https://doi.org/10.1101/2022.06.02.494553; this version posted June 3, 2022. The copyright holder for this preprint (which was not certified by peer review) is the author/funder, who has granted bioRxiv a license to display the preprint in perpetuity. It is made available under aCC-BY-NC-ND 4.0 International license.

DAG and immediately frozen in liquid N_2 for the subsequent isolation of total RNA. The RNA samples of six biological replicates for each accession were equally mixed and were subjected to 150 bp paired-end RNA sequencing with the Illumina HiSeq X Ten platform. In addition, at the 4, 7, and 14 DAG, the six root samples per biological replicate were collected to measure the total root length, root surface, root volume, and root diameter using the Wseen LA-S image system (Hangzhou Wseen Testing Technology Co. LTD). Meanwhile, the root number, primary root length, and root/leaf fresh weight were manually measured.

RNA-Seq data mapping and SNP calling

Raw RNA-Seq reads were filtered to remove sequencing adapters and low-quality bases using Trimmomatic (v0.33) (Bolger et al., 2014) with default parameters. The filtered reads were firstly aligned to bread wheat reference genome sequence (IWGSC RefSeq v1.0) using the STAR software (v2.4.2a)(Dobin et al., 2013) with the 2-pass mapping mode. Then, the filtered reads were mapped to the transcriptome sequence (IWGSC RefSeq v1.1 annotation) with BWA (v0.7.17) (Li and Durbin, 2010). The unique mapping RNA-Seq reads with coincident mapping locations between genome and transcriptome mapping procedures were collected to reduce mapping error and used for the subsequential SNP calling.

A two-step procedure that carefully considered RNA-seq data characteristics was employed to detect SNPs referring to reported method (Fu et al., 2013). Firstly, raw SNPs were called with a population SNP-calling manner referring to the best practices of GATK (v4.0.2.0) (McKenna et al., 2010) and were filtered with the following parameters: (1) mapping quality ≥ 40, SNP quality ≥ 30, genotype quality for each accession ≥ 20, QD (SNP quality/reads depth) ≥ 2; (2) each SNP was more than five bp away from an InDel; (3) for homozygous genotypes, the supporting reads had to be equal to or greater than five for each accession; (4) for heterozygous genotypes, the supporting reads for both the reference and alternative alleles had to be equal to or greater than three for each accession. The SNPs that failed to pass the above

bioRxiv preprint doi: https://doi.org/10.1101/2022.06.02.494553; this version posted June 3, 2022. The copyright holder for this preprint (which was not certified by peer review) is the author/funder, who has granted bioRxiv a license to display the preprint in perpetuity. It is made available under aCC-BY-NC-ND 4.0 International license.

parameters were assigned as missing. Secondly, to further exclude possible false polymorphic sites caused by intrinsic mapping errors, we simulated RNA-seq read sequences based on the whole wheat transcriptome without mutation introduction, aligned these sequences to the reference and identified SNPs using the same strategies as in the first step to produce a mapping error SNP set. Any SNPs that matched the mapping error SNP set were removed. The high-quality SNPs were annotated using the SnpEff (v4.3) (Cingolani et al., 2012).

SNP imputation and accuracy evaluation

The beagle (v5.1) (Browning et al., 2018) was used to impute missing genotypes. To get the optimal imputation accuracy and filling rate, we randomly masked 10750 sites with missing rates varied from 10 to 90% and found that the imputation accuracy of masked sites was more than 99% when the missing rate was < 0.8 (Table S12). Therefore, SNPs with the missing rate < 0.8 were imputed.

To evaluate the reproducibility of our pipeline and the accuracy of the final SNPs, we firstly compared the identified genotypes of two biological replicates of three accessions. It showed an average of 98.85% concordant rate between replicates of each accession, indicating our SNP calling pipeline was high reproducibility (Table S13). Secondly, only 387 alternative alleles (0.09%) were detected in the wheat cv. Chinese Spring that was used to generate the reference genome sequence, suggesting a low false-positive rate of our pipeline. Thirdly, four accessions were selected to genotype with wheat 660 K SNP arrays, and the results showed the accuracy was more than 99% and 94.32% before and after SNP imputation, respectively (Table S14). Overall, despite the hexaploidy nature and more than 85% repetitive DNA of bread wheat genome, the above data indicated that the reproducibility of our SNP calling pipeline and the accuracy of the identified SNPs in the current study is high enough. The code of our SNP calling pipeline could be downloaded from https://github.com/biozhp/root_rnaseq.

bioRxiv preprint doi: https://doi.org/10.1101/2022.06.02.494553; this version posted June 3, 2022. The copyright holder for this preprint (which was not certified by peer review) is the author/funder, who has granted bioRxiv a license to display the preprint in perpetuity. It is made available under aCC-BY-NC-ND 4.0 International license.

Population genetic analysis

To classify the accessions, our SNP data were merged with the recently published SNP data of hexaploidy accessions downloaded from the National Genomics Data Center (https://bigd.big.ac.cn/gvm, GVM000082) (Zhou et al., 2020). The shared SNPs between our results and the *Triticum* population sequencing project were used to construct a phylogenetic tree using RAxML (v8.2.12) (Stamatakis, 2014) with the parameters: -f a -m GTRGAMMA -p 12346 -x 12346 -# 100. The phylogenetic tree initially divided our wheat accessions into LA and CV groups, referring to the determined classification in the *Triticum* sequencing project. Then, 34 accessions with conflict classifications between the phylogenetic tree and pedigree documentation were removed, resulting in 87 LA and 264 MC for the subsequent analysis. The phylogenetic tree was visualised by iTOL (v6) (Letunic and Bork, 2021).

The imputed SNPs with MAF > 0.05 were used to quantify the genome-wide population structure and infer population structure with ADMIXTURE (v1.3.0) (Alexander et al., 2009).

Gene expression quantification

The filtered reads were aligned to the high and low confidence transcripts (IWGSC RefSeq v1.1 annotation) using the kallisto (v0.46.2) (Bray et al., 2016) and summarized expression levels (Transcripts Per Million, TPM) from the transcript level to the gene level using tximport (v1.14.0) (Soneson et al., 2015) with the option 'lengthScaledTPM' referring to the reported method (Ramirez-Gonzalez et al., 2018). To investigate the extent of gene expression variation among the population, the fold change of the TPM at 95th percentiles to that of the 5th percentiles (TPM > 0.5) in the whole population was calculated.

Identification of differentially expressed genes

bioRxiv preprint doi: https://doi.org/10.1101/2022.06.02.494553; this version posted June 3, 2022. The copyright holder for this preprint (which was not certified by peer review) is the author/funder, who has granted bioRxiv a license to display the preprint in perpetuity. It is made available under aCC-BY-NC-ND 4.0 International license.

For each gene, the significance of expression difference between the two compared groups was calculated with the Wilcoxon rank-sum test (Li et al., 2022). Genes with FDR adjusted *P-value* < 0.01 were considered as candidate DEGs. Then, to exclude the effects of population structure on DEG detection, the 100 random permutations were performed by randomly sampling 60% accessions from each of the two compared groups and further randomly removing accessions from the larger size group to reach the same size as the smaller group. The observation number of each DEG in the 100 random permutations was recorded. The DEGs with an observation number of more than ten times were considered reliable DEGs and used for further analysis. For investigating the expected observation numbers of DEGs, we performed 100,000 permutations by randomly sampling accessions from the whole population to construct two same size groups as LA and CV, and found that only 0.2% of the tests had DEGs, and the 95% confidence interval of the observation numbers of DEGs was from 0 to 0.27. Therefore, we selected more than ten times as threshold in the DEG detection, which was big enough to exclude the DEGs by chance.

GO enrichment analysis

GO annotation for high confidence genes was downloaded from the Ensembl Plants Genes 49 database, and GO annotation for the low confidence genes were obtained with eggNOG-mapper (v2) (Cantalapiedra et al., 2021). GO enrichment analysis was performed using the R package clusterProfiler (v3.14.3) with the "enricher" function (Yu et al., 2012).

Association analyses

The imputed SNPs with MAF > 0.05 were used for the GWAS analysis with the mixed linear model implemented in GAPIT (Wang and Zhang, 2021). The cutoff for determining significant associations was *P-value* $<1\times10^{-4}$. The genes whose expression values at the 5th percentile were more than 0.5 were filtered out, and their expression levels were normalized using a normal quantile transformation with the

bioRxiv preprint doi: https://doi.org/10.1101/2022.06.02.494553; this version posted June 3, 2022. The copyright holder for this preprint (which was not certified by peer review) is the author/funder, who has granted bioRxiv a license to display the preprint in perpetuity. It is made available under aCC-BY-NC-ND 4.0 International license.

"qqnorm" function in R. The function "cGWAS.emmax" of R package cpgen (v0.2) was used for TWAS analysis (Tang et al., 2021).

Permutations of the phenotyping comparison

To avoid the inference from population structure and kinships between wheat accessions in phenotyping comparisons, randomly sampling 60% accessions from each of the two compared groups and further randomly removing accessions from the larger size group to reach the same size as the smaller group. In the 1000 random permutations, the observation numbers of significant difference with the Student's t-test were recorded.

Identification of co-expressed genes with *Rht-A1/B1/D1*

To identify the co-expression genes with *Rht-A1/B1/D1*, we randomly selected 60% accessions from the *Rht-B1aRht-D1a* (marked NO) group to calculate the Pearson correlation coefficients and *P-value* between the TPM of each candidate gene and the TPM of *Rht-A1/B1/D1* using the "cor.test" function in R. Accordingly, we randomly selected 60% accessions from *Rht-B1bRht-D1a* (marked *B1b*) or *Rht-B1aRht-D1b* (marked *D1b*) groups to identify the co-expression genes with *Rht-B1* or *Rht-D1*, respectively. The genes that were observed more than ten times with *P-value* $< 10^{-10}$ in Pearson's correlation test in the 100 random permutationswere regarded as co-expressed genes.

Gibberellin treatment

The 18 randomly selected accessions from each of the *Rht-B1aRht-D1a*, *Rht-B1bRht-D1a* and *Rht-B1aRht-D1b* genotypes, were treated by exogenous GA (GA_3) in a hydroponic system and soil cultivation system. The plants grown in the hydroponic system were treated with 0.2 and 2 μmol/L GA_3 for eight days after germination, and those cultivated in soil were treated with 15 μmol/L GA_3 for nine days from three DAG. The roots and leaves were collected to measure the primary

bioRxiv preprint doi: https://doi.org/10.1101/2022.06.02.494553; this version posted June 3, 2022. The copyright holder for this preprint (which was not certified by peer review) is the author/funder, who has granted bioRxiv a license to display the preprint in perpetuity. It is made available under aCC-BY-NC-ND 4.0 International license.

root length and leaf length.

Over-expression transgenic vector construction and plant transformation

To overexpress *TaRht-D1b*, the coding region of which was inserted into the pMWB111 vector under the control of its native promoter. The construct was then introduced into the immature embryos of bread wheat cv. Fielder by Agrobacterium tumefaciens mediated transformation, referring to the established protocols (Hayta et al., 2019).

Cytological observation of root and shoot

FV1200 confocal microscope (Olympus, Tokyo, Japan) was used for the cytological observation of roots and shoots. The sample was harvested and fixed in 4% glutaraldehyde (in 12.5 mM cacodylate, pH 6.9), then vacuumed them three times for 30 minutes, after which they were in fixative overnight at room temperature. After fixation, the tissue was dehydrated through a conventional ethanol series for 30 min per step. Then, the tissue was cleared in 2:1 (v/v) benzyl benzoate: benzyl alcohol for a minimum of 1 h. Samples were observed with a confocal microscope under a 488-nm argon laser. ImageJ V1.48 was used to measure the length and width of the cell.

bioRxiv preprint doi: https://doi.org/10.1101/2022.06.02.494553; this version posted June 3, 2022. The copyright holder for this preprint (which was not certified by peer review) is the author/funder, who has granted bioRxiv a license to display the preprint in perpetuity. It is made available under aCC-BY-NC-ND 4.0 International license.

Data availability

The raw RNA-Seq data were deposited in the Sequence Read Archive (https://www.ncbi.nlm.nih.gov/sra) under accession numbers PRJNA838764. Genotypic, transcriptomic and phenotypic data used in this analysis are publicly available from our website (https://iwheat.net/links/).

Supplemental Data

Supplementary Table 1. Information of all accessions in this study.

Supplementary Table 2. Gene ontology enrichment analyses of the highly and lowly expressed genes.

Supplementary Table 3. Gene ontology enrichment analyses of the highly and lowly varied expression genes.

Supplementary Table 4. The identified DEGs between LA and MC groups.

Supplementary Table 5. Gene ontology enrichment analyses of the DEGs between LA and MC.

Supplementary Table 6. Annotation of DEGs, which were observed in all 100 random permutations.

Supplementary Table 7. GWAS results of the root surface and volume at 14 DAGs and the root-shoot ratio at seven DAGs.

Supplementary Table 8. TWAS results of the root surface and volume at 14 DAGs.

Supplementary Table 9. The GWAS results of root surface (14 DAG), volume (14 DAG) and root-shoot ratio (7 DAG) in the population masked Rht-B1b genotypes or masked Rht-D1b genotypes.

bioRxiv preprint doi: https://doi.org/10.1101/2022.06.02.494553; this version posted June 3, 2022. The copyright holder for this preprint (which was not certified by peer review) is the author/funder, who has granted bioRxiv a license to display the preprint in perpetuity. It is made available under aCC-BY-NC-ND 4.0 International license.

Supplementary Table 10. Gene ontology enrichment analyses of the DEGs derived from comparing *D1b* and *NO* genotypes.

Supplementary Table 11. Gene ontology enrichment analyses of the DEGs derived from comparing *B1b* and *NO* genotypes.

Supplementary Table 12. Imputation accuracy of SNPs under different cutoffs of missing rate.

Supplementary Table 13. The reproducibility of our SNP identification pipeline among three biological replications.

Supplementary Table 14. The concordance rate of the identified SNPs with our pipeline and the wheat 660K SNP arrays.

ACKNOWLEDGEMENTS

This work was supported by grants from the National Natural Science Foundation of China (31571756 and 31870298) to SX, the fellowship of China Postdoctoral Science Foundation (2021T140566) to XW. And we thank the crop biology innovation center of college of agronomy (NWAFU) for providing equipment support, the High-Performance Computing (HPC) of Northwest A&F University for providing computing platform.

AUTHOR CONTRIBUTIONS

SX and ZK conceived the project and designed the research. ZK, SX and DH collected wheat accession. XW, PZ, XG, ZL, XM, YZ, XL, LH and WW performed the sample preparation, RNA sequencing and phenotypic data collection and process. SX, XW, PZ, XG organized the data and wrote the manuscript. All authors discussed the results and commented on the manuscript. All authors read and approved the final manuscript.

REFERENCES

bioRxiv preprint doi: https://doi.org/10.1101/2022.06.02.494553; this version posted June 3, 2022. The copyright holder for this preprint (which was not certified by peer review) is the author/funder, who has granted bioRxiv a license to display the preprint in perpetuity. It is made available under aCC-BY-NC-ND 4.0 International license.

Abbo, S., Pinhasi van-Oss, R., Gopher, A., Saranga, Y., Ofner, I., Peleg, Z. (2014). Plant domestication versus crop evolution: a conceptual framework for cereals and grain legumes. Trends Plant Sci **19,** 351-360.

Alexander, D.H., Novembre, J., Lange, K. (2009). Fast model-based estimation of ancestry in unrelated individuals. Genome Res **19,** 1655-1664.

Azodi, C.B., Pardo, J., VanBuren, R., de Los Campos, G., Shiu, S.H. (2020). Transcriptome-Based Prediction of Complex Traits in Maize. Plant Cell **32,** 139-151.

Bacher, H., Zhu, F., Gao, T., Liu, K., Dhatt, B.K., Awada, T., Zhang, C., Distelfeld, A., Yu, H., Peleg, Z., Walia, H. (2021). Wild emmer introgression alters root-to-shoot growth dynamics in durum wheat in response to water stress. Plant Physiol **187,** 1149-1162.

Binenbaum, J., Weinstain, R., Shani, E. (2018). Gibberellin Localization and Transport in Plants. Trends Plant Sci **23,** 410-421.

Bolger, A.M., Lohse, M., Usadel, B. (2014). Trimmomatic: a flexible trimmer for Illumina sequence data. Bioinformatics **30,** 2114-2120.

Bray, N.L., Pimentel, H., Melsted, P., Pachter, L. (2016). Near-optimal probabilistic RNA-seq quantification. Nat Biotechnol **34,** 525-527.

Browning, B.L., Zhou, Y., Browning, S.R. (2018). A One-Penny Imputed Genome from Next-Generation Reference Panels. Am J Hum Genet **103,** 338-348.

Bulik-Sullivan, B., Finucane, H.K., Anttila, V., Gusev, A., Day, F.R., Loh, P.R., Duncan, L., Perry, J.R., Patterson, N., Robinson, E.B., Daly, M.J., Price, A.L., Neale, B.M. (2015). An atlas of genetic correlations across human diseases and traits. Nat Genet **47,** 1236-1241.

Calleja-Cabrera, J., Boter, M., Oñate-Sánchez, L., Pernas, M. (2020). Root Growth Adaptation to Climate Change in Crops. Front Plant Sci **11,** 544.

Cantalapiedra, C.P., Hernandez-Plaza, A., Letunic, I., Bork, P., Huerta-Cepas, J. (2021). eggNOG-mapper v2: Functional Annotation, Orthology Assignments, and Domain Prediction at the Metagenomic Scale. Mol Biol Evol **38,** 5825-5829.

Chen, J.H., Jiang, H.W., Hsieh, E.J., Chen, H.Y., Chien, C.T., Hsieh, H.L., Lin, T.P. (2012). Drought and salt stress tolerance of an Arabidopsis glutathione S-transferase U17 knockout mutant are attributed to the combined effect of glutathione and abscisic acid. Plant Physiol **158,** 340-351.

Chen, W., Wu, Y., Zheng, Z., Qi, T., Visscher, P.M., Zhu, Z., Yang, J. (2021). Improved analyses of GWAS summary statistics by reducing data heterogeneity and errors. Nat Commun **12,** 7117.

Cingolani, P., Platts, A., Wang le, L., Coon, M., Nguyen, T., Wang, L., Land, S.J., Lu, X., Ruden, D.M. (2012). A program for annotating and predicting the effects of single nucleotide polymorphisms, SnpEff: SNPs in the genome of Drosophila melanogaster strain w1118; iso-2; iso-3. Fly (Austin) **6,** 80-92.

D'Alessandro, S., Golin, S., Hardtke, C.S., Lo Schiavo, F., Zottini, M. (2015). The co-chaperone p23 controls root development through the modulation of auxin distribution in the Arabidopsis root meristem. J Exp Bot **66,** 5113-5122.

De Smet, I., Vassileva, V., De Rybel, B., Levesque, M.P., Grunewald, W., Van Damme, D., Van Noorden, G., Naudts, M., Van Isterdael, G., De Clercq, R., Wang, J.Y., Meuli, N., Vanneste, S., Friml, J., Hilson, P., Jürgens, G., Ingram, G.C., Inzé, D., Benfey, P.N.,

bioRxiv preprint doi: https://doi.org/10.1101/2022.06.02.494553; this version posted June 3, 2022. The copyright holder for this preprint (which was not certified by peer review) is the author/funder, who has granted bioRxiv a license to display the preprint in perpetuity. It is made available under aCC-BY-NC-ND 4.0 International license.

Beeckman, T. (2008). Receptor-like kinase ACR4 restricts formative cell divisions in the Arabidopsis root. Science **322,** 594-597.

de Vries, F.T., Griffiths, R.I., Knight, C.G., Nicolitch, O., Williams, A. (2020). Harnessing rhizosphere microbiomes for drought-resilient crop production. Science **368,** 270-274.

Den Herder, G., Van Isterdael, G., Beeckman, T., De Smet, I. (2010). The roots of a new green revolution. Trends Plant Sci **15,** 600-607.

Dobin, A., Davis, C.A., Schlesinger, F., Drenkow, J., Zaleski, C., Jha, S., Batut, P., Chaisson, M., Gingeras, T.R. (2013). STAR: ultrafast universal RNA-seq aligner. Bioinformatics **29,** 15-21.

Fauman, E.B. (2020). Current Techniques for Complex Phenotypes: GWAS of the Electrocardiogram. Trends Genet **36,** 897-899.

Fu, J., Cheng, Y., Linghu, J., Yang, X., Kang, L., Zhang, Z., Zhang, J., He, C., Du, X., Peng, Z., Wang, B., Zhai, L., Dai, C., Xu, J., Wang, W., Li, X., Zheng, J., Chen, L., Luo, L., Liu, J., Qian, X., Yan, J., Wang, J., Wang, G. (2013). RNA sequencing reveals the complex regulatory network in the maize kernel. Nat Commun **4,** 2832.

Gao, Z., Shi, Z., Zhang, A., Guo, J. (2015). Distribution of genes associated with yield potential and water-saving in Chinese Zone II wheat detected by developed functional markers. Journal of genetics **94,** 35-42.

Gilliland, L.U., Pawloski, L.C., Kandasamy, M.K., Meagher, R.B. (2003). Arabidopsis actin gene ACT7 plays an essential role in germination and root growth. The Plant Journal **33,** 319-328.

Godfray, H.C., Beddington, J.R., Crute, I.R., Haddad, L., Lawrence, D., Muir, J.F., Pretty, J., Robinson, S., Thomas, S.M., Toulmin, C. (2010). Food security: the challenge of feeding 9 billion people. Science **327,** 812-818.

Golan, G., Hendel, E., Méndez Espitia, G.E., Schwartz, N., Peleg, Z. (2018). Activation of seminal root primordia during wheat domestication reveals underlying mechanisms of plant resilience. Plant Cell Environ **41,** 755-766.

Guedira, M., Brown-Guedira, G., Van Sanford, D., Sneller, C., Souza, E., Marshall, D. (2010). Distribution of Rht Genes in Modern and Historic Winter Wheat Cultivars from the Eastern and Central USA. Crop Sci **50,** 1811-1822.

Hao, C., Jiao, C., Hou, J., Li, T., Liu, H., Wang, Y., Zheng, J., Liu, H., Bi, Z., Xu, F., Zhao, J., Ma, L., Wang, Y., Majeed, U., Liu, X., Appels, R., Maccaferri, M., Tuberosa, R., Lu, H., Zhang, X. (2020). Resequencing of 145 Landmark Cultivars Reveals Asymmetric Sub-genome Selection and Strong Founder Genotype Effects on Wheat Breeding in China. Mol Plant **13,** 1733-1751.

Hayta, S., Smedley, M.A., Demir, S.U., Blundell, R., Hinchliffe, A., Atkinson, N., Harwood, W.A. (2019). An efficient and reproducible *Agrobacterium*-mediated transformation method for hexaploid wheat (*Triticum aestivum* L.). Plant Methods **15,** 121.

Hendel, E., Bacher, H., Oksenberg, A., Walia, H., Schwartz, N., Peleg, Z. (2021). Deciphering the genetic basis of wheat seminal root anatomy uncovers ancestral axial conductance alleles. Plant Cell Environ **44,** 1921-1934.

Hou, L., Zhang, A., Wang, R., Zhao, P., Zhang, D., Jiang, Y., Diddugodage, C.J., Wang, X., Ni, Z., Xu, S. (2019). Brassinosteroid Regulates Root Development with Highly Redundant Genes in Hexaploid Wheat. Plant Cell Physiol **60,** 1761-1777.

bioRxiv preprint doi: https://doi.org/10.1101/2022.06.02.494553; this version posted June 3, 2022. The copyright holder for this preprint (which was not certified by peer review) is the author/funder, who has granted bioRxiv a license to display the preprint in perpetuity. It is made available under aCC-BY-NC-ND 4.0 International license.

Hu, Y., Chen, J., Fang, L., Zhang, Z., Ma, W., Niu, Y., Ju, L., Deng, J., Zhao, T., Lian, J., Baruch, K., Fang, D., Liu, X., Ruan, Y.L., Rahman, M.U., Han, J., Wang, K., Wang, Q., Wu, H., Mei, G., Zang, Y., Han, Z., Xu, C., Shen, W., Yang, D., Si, Z., Dai, F., Zou, L., Huang, F., Bai, Y., Zhang, Y., Brodt, A., Ben-Hamo, H., Zhu, X., Zhou, B., Guan, X., Zhu, S., Chen, X., Zhang, T. (2019). Gossypium barbadense and Gossypium hirsutum genomes provide insights into the origin and evolution of allotetraploid cotton. Nat Genet **51,** 739-748.

International Wheat Genome Sequencing Consortium (IWGSC) (2018). Shifting the limits in wheat research and breeding using a fully annotated reference genome. Science **361,** 6403.

Khan, M.A., Gemenet, D.C., Villordon, A. (2016). Root System Architecture and Abiotic Stress Tolerance: Current Knowledge in Root and Tuber Crops. Front Plant Sci **7,** 1584.

Kremling, K.A.G., Diepenbrock, C.H., Gore, M.A., Buckler, E.S., Bandillo, N.B. (2019). Transcriptome-Wide Association Supplements Genome-Wide Association in *Zea mays*. G3 (Bethesda) **9,** 3023-3033.

Lanning, S.P., Martin, J.M., Stougaard, R.N., Guillen-Portal, F.R., Talbert, L.E. (2012). Evaluation of Near-Isogenic Lines for Three Height-Reducing Genes in Hard Red Spring Wheat. Crop Sci **52,** 1145-1152.

Lee, B.H., Ko, J.H., Lee, S., Lee, Y., Pak, J.H., Kim, J.H. (2009). The Arabidopsis GRF-INTERACTING FACTOR gene family performs an overlapping function in determining organ size as well as multiple developmental properties. Plant Physiol **151,** 655-668.

Letunic, I., Bork, P. (2021). Interactive Tree Of Life (iTOL) v5: an online tool for phylogenetic tree display and annotation. Nucleic Acids Res **49,** W293-2296.

Li, H., Durbin, R. (2010). Fast and accurate long-read alignment with Burrows-Wheeler transform. Bioinformatics **26,** 589-595.

Li, Y., Ge, X., Peng, F., Li, W., Li, J.J. (2022). Exaggerated false positives by popular differential expression methods when analyzing human population samples. Genome Biol **23,** 79.

Liu, Q., Wu, K., Harberd, N.P., Fu, X. (2021). Green Revolution DELLAs: From translational reinitiation to future sustainable agriculture. Mol Plant **14,** 547-549.

Lynch, J. (1995). Root Architecture and Plant Productivity. Plant Physiol **109,** 7-13.

Lynch, J.P. (2007). Roots of the Second Green Revolution. Australian Journal of Botany **55,** 493-512.

McKenna, A., Hanna, M., Banks, E., Sivachenko, A., Cibulskis, K., Kernytsky, A., Garimella, K., Altshuler, D., Gabriel, S., Daly, M., DePristo, M.A. (2010). The Genome Analysis Toolkit: a MapReduce framework for analyzing next-generation DNA sequencing data. Genome Res **20,** 1297-1303.

Ohashi-Ito, K., Fukuda, H. (2003). HD-zip III homeobox genes that include a novel member, ZeHB-13 (Zinnia)/ATHB-15 (Arabidopsis), are involved in procambium and xylem cell differentiation. Plant Cell Physiol **44,** 1350-1358.

Pearce, S., Saville, R., Vaughan, S.P., Chandler, P.M., Wilhelm, E.P., Sparks, C.A., Al-Kaff, N., Korolev, A., Boulton, M.I., Phillips, A.L., Hedden, P., Nicholson, P., Thomas, S.G. (2011). Molecular characterization of Rht-1 dwarfing genes in hexaploid wheat. Plant Physiol **157,** 1820-1831.

Qin, H., Pandey, B.K., Li, Y., Huang, G., Wang, J., Quan, R., Zhou, J., Zhou, Y., Miao, Y., Zhang, D., Bennett, M.J., Huang, R. (2022). Orchestration of ethylene and gibberellin signals

bioRxiv preprint doi: https://doi.org/10.1101/2022.06.02.494553; this version posted June 3, 2022. The copyright holder for this preprint (which was not certified by peer review) is the author/funder, who has granted bioRxiv a license to display the preprint in perpetuity. It is made available under aCC-BY-NC-ND 4.0 International license.

692 determines primary root elongation in rice. Plant Cell **34,** 1273-1288.
693 **Ramirez-Gonzalez, R.H., Borrill, P., Lang, D., Harrington, S.A., Brinton, J., Venturini, L., Davey,**
694 **M., Jacobs, J., van Ex, F., Pasha, A., Khedikar, Y., Robinson, S.J., Cory, A.T., Florio, T.,**
695 **Concia, L., Juery, C., Schoonbeek, H., Steuernagel, B., Xiang, D., Ridout, C.J., Chalhoub,**
696 **B., Mayer, K.F.X., Benhamed, M., Latrasse, D., Bendahmane, A., International Wheat**
697 **Genome Sequencing, C., Wulff, B.B.H., Appels, R., Tiwari, V., Datla, R., Choulet, F.,**
698 **Pozniak, C.J., Provart, N.J., Sharpe, A.G., Paux, E., Spannagl, M., Brautigam, A., Uauy,**
699 **C.** (2018). The transcriptional landscape of polyploid wheat. Science **361,** 6403.
700 **Rizza, A., Jones, A.M.** (2019). The makings of a gradient: spatiotemporal distribution of gibberellins
701 in plant development. Curr Opin Plant Biol **47,** 9-15.
702 **Shani, E., Weinstain, R., Zhang, Y., Castillejo, C., Kaiserli, E., Chory, J., Tsien, R.Y., Estelle, M.**
703 (2013). Gibberellins accumulate in the elongating endodermal cells of Arabidopsis root. Proc
704 Natl Acad Sci U S A **110,** 4834-4839.
705 **Sherman, J.D., Nash, D., Lanning, S.P., Martin, J.M., Blake, N.K., Morris, C.F., Talbert, L.E.**
706 (2014). Genetics of End-Use Quality Differences between a Modern and Historical Spring
707 Wheat. Crop Sci **54,** 1972-1980.
708 **Snowdon, R.J., Wittkop, B., Chen, T.W., Stahl, A.** (2020). Crop adaptation to climate change as a
709 consequence of long-term breeding. Theor Appl Genet **134,** 1613-1623.
710 **Soneson, C., Love, M.I., Robinson, M.D.** (2015). Differential analyses for RNA-seq: transcript-level
711 estimates improve gene-level inferences. F1000Res **4,** 1521.
712 **Stamatakis, A.** (2014). RAxML version 8: a tool for phylogenetic analysis and post-analysis of large
713 phylogenies. Bioinformatics **30,** 1312-1313.
714 **Tang, S., Zhao, H., Lu, S., Yu, L., Zhang, G., Zhang, Y., Yang, Q.Y., Zhou, Y., Wang, X., Ma, W.,**
715 **Xie, W., Guo, L.** (2021). Genome- and transcriptome-wide association studies provide
716 insights into the genetic basis of natural variation of seed oil content in Brassica napus. Mol
717 Plant **14,** 470-487.
718 **Tanimoto, E.** (2012). Tall or short? Slender or thick? A plant strategy for regulating elongation growth
719 of roots by low concentrations of gibberellin. Ann Bot **110,** 373-381.
720 **Teotia, S., Lamb, R.S.** (2011). RCD1 and SRO1 are necessary to maintain meristematic fate in
721 Arabidopsis thaliana. J Exp Bot **62,** 1271-1284.
722 **Topham, A.T., Taylor, R.E., Yan, D., Nambara, E., Johnston, I.G., Bassel, G.W.** (2017).
723 Temperature variability is integrated by a spatially embedded decision-making center to break
724 dormancy in Arabidopsis seeds. Proc Natl Acad Sci U S A **114,** 6629-6634.
725 **Truernit, E., Siemering, K.R., Hodge, S., Grbic, V., Haseloff, J.** (2006). A map of KNAT gene
726 expression in the Arabidopsis root. Plant Mol Biol **60,** 1-20.
727 **Van De Velde, K., Thomas, S.G., Heyse, F., Kaspar, R., Van Der Straeten, D., Rohde, A.** (2021).
728 N-terminal truncated RHT-1 proteins generated by translational reinitiation cause
729 semi-dwarfing of wheat Green Revolution alleles. Mol Plant **14,** 679-687.
730 **van de Wouw, M., van Hintum, T., Kik, C., van Treuren, R., Visser, B.** (2010). Genetic diversity
731 trends in twentieth century crop cultivars: a meta analysis. Theor Appl Genet **120,** 1241-1252.
732 **van der Bom, F.J.T., Williams, A., Bell, M.J.** (2020). Root architecture for improved resource capture:
733 trade-offs in complex environments. J Exp Bot **71,** 5752-5763.

bioRxiv preprint doi: https://doi.org/10.1101/2022.06.02.494553; this version posted June 3, 2022. The copyright holder for this preprint (which was not certified by peer review) is the author/funder, who has granted bioRxiv a license to display the preprint in perpetuity. It is made available under aCC-BY-NC-ND 4.0 International license.

Wainberg, M., Sinnott-Armstrong, N., Mancuso, N., Barbeira, A.N., Knowles, D.A., Golan, D., Ermel, R., Ruusalepp, A., Quertermous, T., Hao, K., Björkegren, J.L.M., Im, H.K., Pasaniuc, B., Rivas, M.A., Kundaje, A. (2019). Opportunities and challenges for transcriptome-wide association studies. Nat Genet **51,** 592-599.

Wang, J., Zhang, Z. (2021). GAPIT Version 3: Boosting Power and Accuracy for Genomic Association and Prediction. Genomics Proteomics Bioinformatics **19,** 629-640.

Watt, M., Magee, L.J., McCully, M.E. (2008). Types, structure and potential for axial water flow in the deepest roots of field-grown cereals. New Phytol **178,** 135-146.

Wu, J., Kong, X., Wan, J., Liu, X., Zhang, X., Guo, X., Zhou, R., Zhao, G., Jing, R., Fu, X., Jia, J. (2011). Dominant and pleiotropic effects of a GAI gene in wheat results from a lack of interaction between DELLA and GID1. Plant Physiol **157,** 2120-2130.

Wu, Y., Chang, Y., Luo, L., Tian, W., Gong, Q., Liu, X. (2022). Abscisic acid employs NRP-dependent PIN2 vacuolar degradation to suppress auxin-mediated primary root elongation in Arabidopsis. New Phytol **233,** 297-312.

Wu, Y., Thorne, E.T., Sharp, R.E., Cosgrove, D.J. (2001). Modification of expansin transcript levels in the maize primary root at low water potentials. Plant Physiol **126,** 1471-1479.

Wurschum, T., Langer, S.M., Longin, C.F. (2015). Genetic control of plant height in European winter wheat cultivars. TAG. Theoretical and applied genetics. Theor Appl Genet **128,** 865-874.

Wurschum, T., Langer, S.M., Longin, C.F.H., Tucker, M.R., and Leiser, W.L. (2017). A modern Green Revolution gene for reduced height in wheat. Plant J **92,** 892-903.

Wurschum, T., Liu, G., Boeven, P.H.G., Longin, C.F.H., Mirdita, V., Kazman, E., Zhao, Y., Reif, J.C. (2018). Exploiting the Rht portfolio for hybrid wheat breeding. Theor Appl Genet **131,** 1433-1442.

Yokoyama, A., Yamashino, T., Amano, Y., Tajima, Y., Imamura, A., Sakakibara, H., Mizuno, T. (2007). Type-B ARR transcription factors, ARR10 and ARR12, are implicated in cytokinin-mediated regulation of protoxylem differentiation in roots of Arabidopsis thaliana. Plant Cell Physiol **48,** 84-96.

Yu, G., Wang, L.G., Han, Y., He, Q.Y. (2012). clusterProfiler: an R package for comparing biological themes among gene clusters. OMICS **16,** 284-287.

Yue, K., Sandal, P., Williams, E.L., Murphy, E., Stes, E., Nikonorova, N., Ramakrishna, P., Czyzewicz, N., Montero-Morales, L., Kumpf, R., Lin, Z., van de Cotte, B., Iqbal, M., Van Bel, M., Van De Slijke, E., Meyer, M.R., Gadeyne, A., Zipfel, C., De Jaeger, G., Van Montagu, M., Van Damme, D., Gevaert, K., Rao, A.G., Beeckman, T., De Smet, I. (2016). PP2A-3 interacts with ACR4 and regulates formative cell division in the Arabidopsis root. Proc Natl Acad Sci U S A **113,** 1447-1452.

Zhang, L., Su, W., Tao, R., Zhang, W., Chen, J., Wu, P., Yan, C., Jia, Y., Larkin, R.M., Lavelle, D., Truco, M.J., Chin-Wo, S.R., Michelmore, R.W., Kuang, H. (2017). RNA sequencing provides insights into the evolution of lettuce and the regulation of flavonoid biosynthesis. Nat Commun **8,** 2264.

Zhang, X., Yang, S., Zhou, Y., He, Z., Xia, X. (2006). Distribution of the Rht-B1b, Rht-D1b and Rht8 reduced height genes in autumn-sown Chinese wheats detected by molecular markers. Euphytica **152,** 109-116.

bioRxiv preprint doi: https://doi.org/10.1101/2022.06.02.494553; this version posted June 3, 2022. The copyright holder for this preprint (which was not certified by peer review) is the author/funder, who has granted bioRxiv a license to display the preprint in perpetuity. It is made available under aCC-BY-NC-ND 4.0 International license.

Zhou, Y., Zhao, X., Li, Y., Xu, J., Bi, A., Kang, L., Xu, D., Chen, H., Wang, Y., Wang, Y.G., Liu, S., Jiao, C., Lu, H., Wang, J., Yin, C., Jiao, Y., Lu, F. (2020). Triticum population sequencing provides insights into wheat adaptation. Nat Genet **52,** 1412-1422.

Zubo, Y.O., Blakley, I.C., Yamburenko, M.V., Worthen, J.M., Street, I.H., Franco-Zorrilla, J.M., Zhang, W., Hill, K., Raines, T., Solano, R., Kieber, J.J., Loraine, A.E., Schaller, G.E. (2017). Cytokinin induces genome-wide binding of the type-B response regulator ARR10 to regulate growth and development in Arabidopsis. Proc Natl Acad Sci U S A **114,** E5995-E6004.

bioRxiv preprint doi: https://doi.org/10.1101/2022.06.02.494553; this version posted June 3, 2022. The copyright holder for this preprint (which was not certified by peer review) is the author/funder, who has granted bioRxiv a license to display the preprint in perpetuity. It is made available under aCC-BY-NC-ND 4.0 International license.

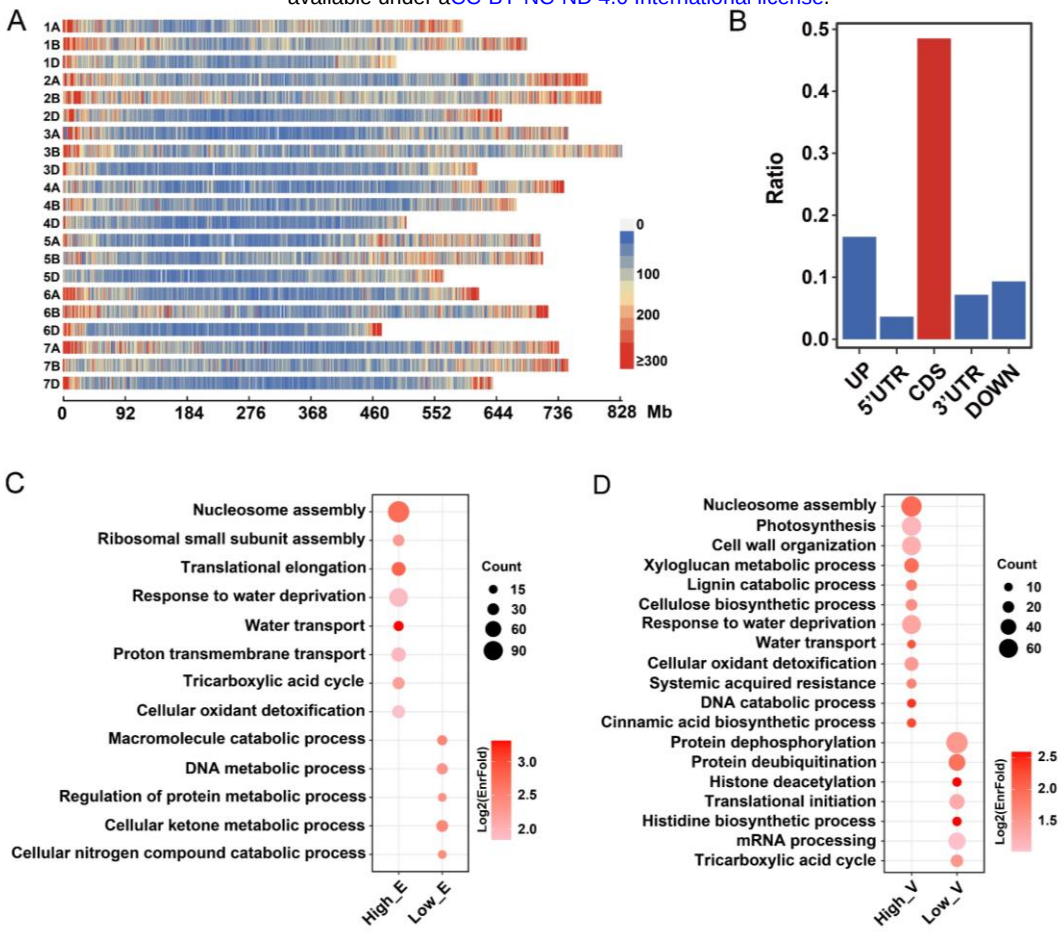

Figure 1. Root transcriptome characteristic of the bread wheat population.

(A) Distribution of the identified SNPs in bread wheat genome. The colour key indicates the number of markers within a window size of 1 Mb.

(B) Distribution of the identified SNPs in gene regions. “UP” and “DOWN” represent the up- and down-stream 5 Kb regions of the annotated genes.

(C) GO analyses of the root highly and lowly expressed genes (the averages of the expression values among the population are in the top and bottom 5%, respectively). The full list of enriched terms is included in Supplemental Table S2.

(D) GO analyses of the highly varied expression genes (fold change from >8) and lowly varied expression genes (fold change from <2) in the population. The fold change is the ratio of TPM at the 95th percentile to that of the 5th percentile. The full list of enriched terms is included in Supplemental Table S3.

bioRxiv preprint doi: https://doi.org/10.1101/2022.06.02.494553; this version posted June 3, 2022. The copyright holder for this preprint (which was not certified by peer review) is the author/funder, who has granted bioRxiv a license to display the preprint in perpetuity. It is made available under aCC-BY-NC-ND 4.0 International license.

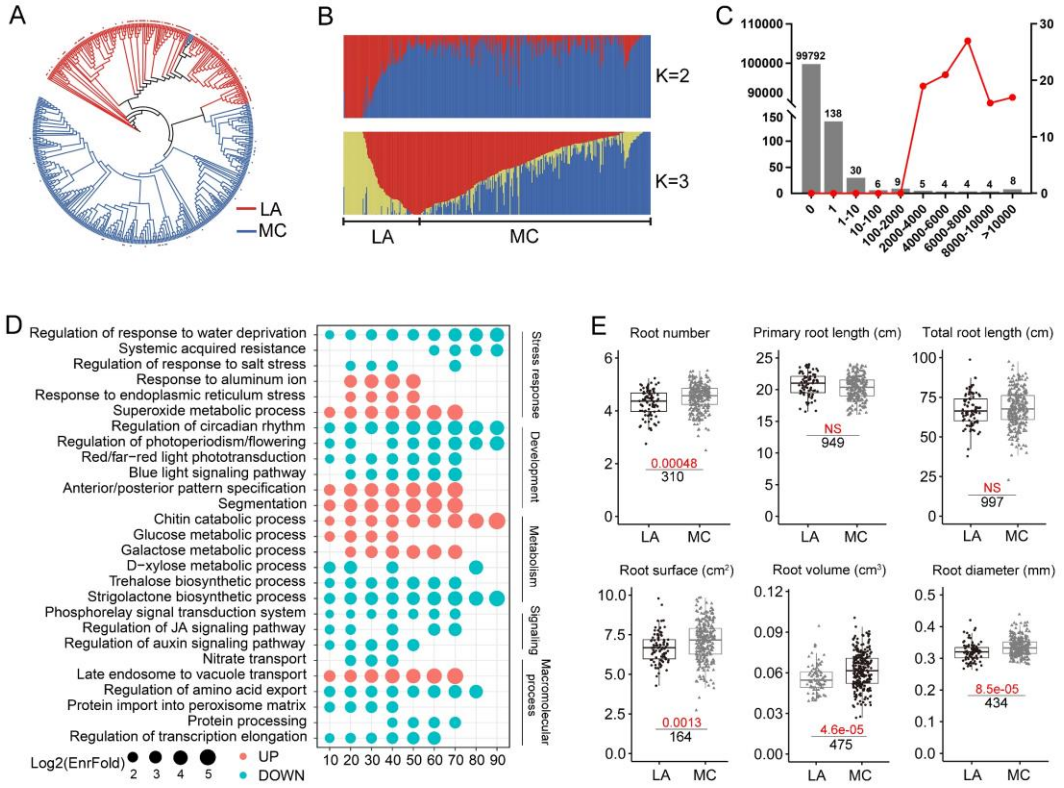

Figure 2. Modern cultivars reshaped the wheat root transcriptome and root development.

(A) Classification of the MC (modern cultivars) and LA (landraces). Phylogenetic trees were constructed based on shared SNPs between our results and the *Triticum* sequencing project. The outer dots represent the varieties which were included in the *Triticum* sequencing project and were coloured based on their classification in this project. These varieties were used as markers to classify the accessions used in our analysis. The phylogenetic clads are coloured based on the pedigree documentation. The accessions with conflict classifications between the *Triticum* sequencing project and pedigree documentation were removed in the following analysis.

(B) The population structure analysis of all accessions with K = 2 and K = 3. Each bar represents an accession, and the different colours correspond to the proportion of different groups.

(C) The distribution of DEGs and observation numbers in the permutations. The X-axis represents the number of DEGs. The left Y-axis and bar plot indicate the numbers of tests in the 100,000 permutations by randomly sampling accessions from the whole population to construct two same size groups as LA and MC. For example, the leftmost bar represents there are 99,792 tests in which the detected DEG number is zero. The right Y-axis and red line represent the numbers of tests in the 100 permutations by randomly sampling 60% accessions from each of the LA and MC groups.

bioRxiv preprint doi: https://doi.org/10.1101/2022.06.02.494553; this version posted June 3, 2022. The copyright holder for this preprint (which was not certified by peer review) is the author/funder, who has granted bioRxiv a license to display the preprint in perpetuity. It is made available under aCC-BY-NC-ND 4.0 International license.

For example, the rightmost dot represents there are 17 tests in which the number of detected DEGs more than 10,000.

(D) GO enrichment analyses of DEGs between LA and MC groups. The X-axis represents the observation numbers of DEGs in the 100 permutations. The full list of enriched terms is included in Supplemental Table S5.

(E) Comparisons of root number, primary root length, total root length, root surface, root volume, and root diameter between LA and MC groups. The red numbers represent *p-values* with Student's t-test using all samples from LA and MC groups, and the "NS" indicates *P-value* > 0.01. The black numbers indicate the observed number of *P-value* < 0.01 in the 1,000 permutations by randomly sampling 60% of the accessions from each of the LA and MC groups and further randomly removing some accessions from MC to reach the same group size as LA.

bioRxiv preprint doi: https://doi.org/10.1101/2022.06.02.494553; this version posted June 3, 2022. The copyright holder for this preprint (which was not certified by peer review) is the author/funder, who has granted bioRxiv a license to display the preprint in perpetuity. It is made available under aCC-BY-NC-ND 4.0 International license.

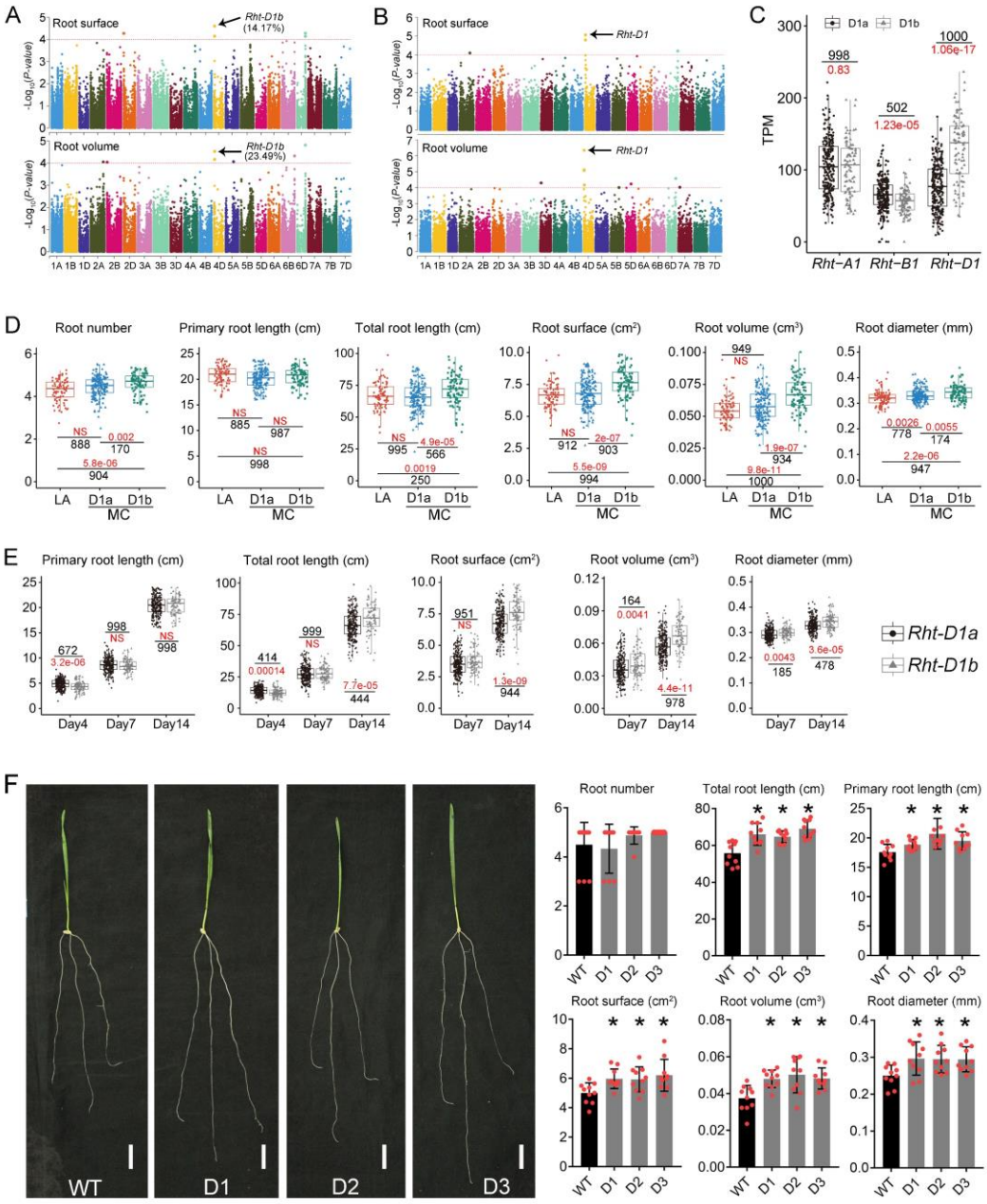

Figure 3. The *Rht-D1b* contributes to the bigger root volume and surface.

(A-B) Manhattan plots of GWAS and TWAS analysis of the root surface and root volume. The number represents the phenotypic variance explained by the indicated SNP.

(C) Comparison of *Rht-A1*, *Rht-B1* and *Rht-D1* expression levels between *Rht-D1a* and *Rht-D1b* genotypes.

(D) Comparison of root number, primary root length, total root length, root surface, root volume and root diameter between LA, *Rht-D1a* contained MC, and *Rht-D1b* contained MC at 14 DAGs.

(E) Comparison of primary root length, total root length, root surface, root volume and root diameter

bioRxiv preprint doi: https://doi.org/10.1101/2022.06.02.494553; this version posted June 3, 2022. The copyright holder for this preprint (which was not certified by peer review) is the author/funder, who has granted bioRxiv a license to display the preprint in perpetuity. It is made available under aCC-BY-NC-ND 4.0 International license.

between *Rht-D1a* and *Rht-D1b* genotypes at four, seven and 14 DAGs. In **(C-E)**, the red numbers represent *p-values* with Student's t-test using all samples from the two compared groups, and the "NS" indicates *P-value* > 0.01. The black numbers indicate the observed number of *P-value* < 0.01 in the 1,000 permutations by randomly sampling 60% of the accessions from each of the two compared groups and further randomly removing accessions from the larger size group to reach the same group size as the smaller one.

(F) The phenotypes and statistical data of root related traits of WT and transgenic lines of *pRht-D1*::*Rht-D1*$^{Rht\text{-}D1b}$ (D1/D2/D3) at 14 DAGs. Scale bar = 2 cm. * indicates Student's t-test *P-value* < 0.05.

bioRxiv preprint doi: https://doi.org/10.1101/2022.06.02.494553; this version posted June 3, 2022. The copyright holder for this preprint (which was not certified by peer review) is the author/funder, who has granted bioRxiv a license to display the preprint in perpetuity. It is made available under aCC-BY-NC-ND 4.0 International license.

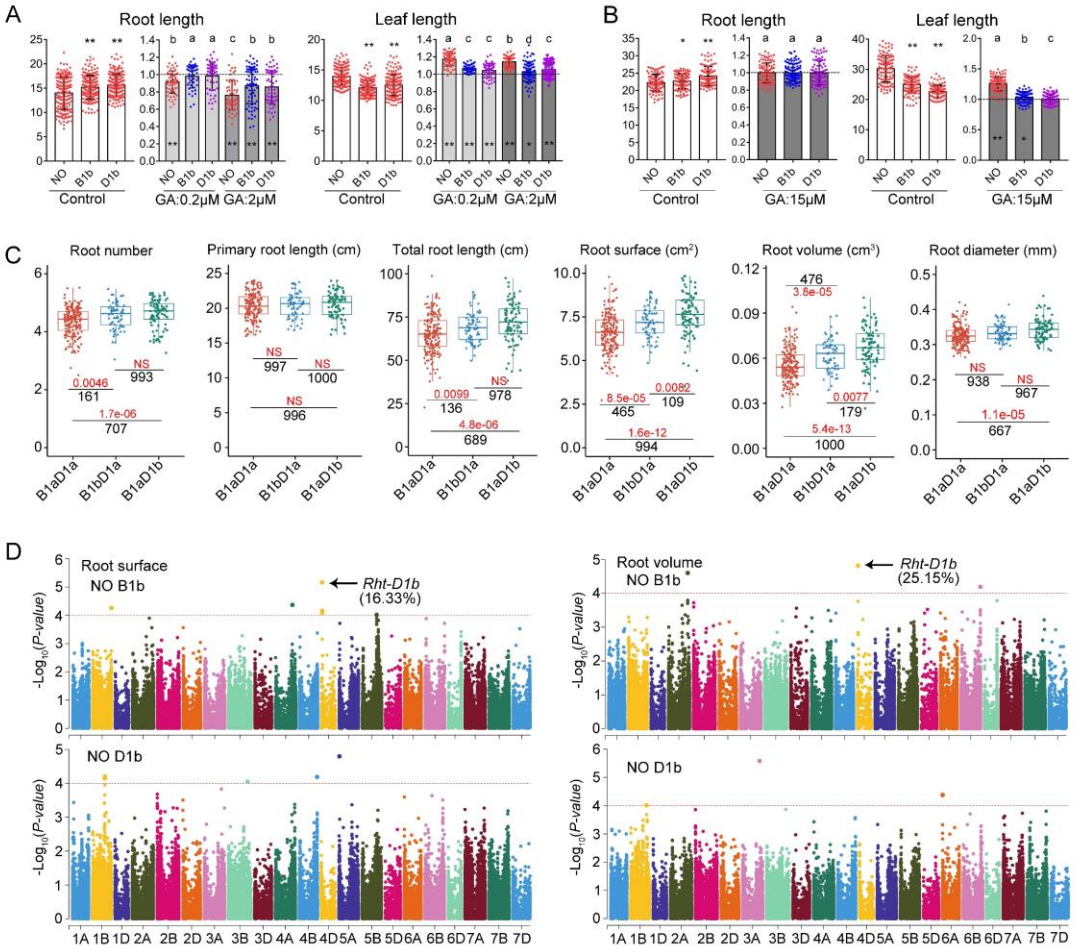

Figure 4. The effects of *Rht-D1b* on root development depend on the GA signaling.

(A-B) The responses of "NO" (*Rht-B1aRht-D1a* genotypes), "B1b" (*Rht-B1bRht-D1a* genotypes) and "D1b" (*Rht-B1aRht-D1b* genotypes) to GA treatment in hydroponics (A) and soil (B) cultivation systems. Under the control condition, * and ** indicates Student's t-test *P-value* < 0. 05 and 0.01, respectively. For the GA treatment experiments, the Y-axis indicates the ratio of phenotyping values under the GA treatment condition to that under the control condition. The asterisk in each column indicates the significant difference compared with the respective control. The letters on the top indicate the significant difference with Student's t-test analysis, *P-value* < 0. 05.

(C) Comparison of root number, primary root length, total root length, root surface, root volume and root diameter between *Rht-B1aRht-D1a* (*B1aD1a*), *Rht-B1bRht-D1a* (*B1bD1a*) and *Rht-B1aRht-D1b* (*B1aD1b*) genotypes. The red numbers represent *p-values* with Student's t-test using all samples from the two compared groups, and the "NS" indicates *P-value* > 0.01. The black numbers indicate the observed number of *P-value* < 0.01 in the 1,000 permutations by randomly sampling 60% of the accessions from each of the two compared groups and further randomly

bioRxiv preprint doi: https://doi.org/10.1101/2022.06.02.494553; this version posted June 3, 2022. The copyright holder for this preprint (which was not certified by peer review) is the author/funder, who has granted bioRxiv a license to display the preprint in perpetuity. It is made available under aCC-BY-NC-ND 4.0 International license.

removing accessions from the larger size group to reach the same group size as the smaller one.

(D) Manhattan plots of GWAS analysis of the root surface and root volume. "NO D1b" and "NO D1b" indicates missed *Rht-B1b* and *Rht-D1b* population used to perform GWAS analysis. The number represents the phenotypic variance explained by the indicated SNP.

bioRxiv preprint doi: https://doi.org/10.1101/2022.06.02.494553; this version posted June 3, 2022. The copyright holder for this preprint (which was not certified by peer review) is the author/funder, who has granted bioRxiv a license to display the preprint in perpetuity. It is made available under aCC-BY-NC-ND 4.0 International license.

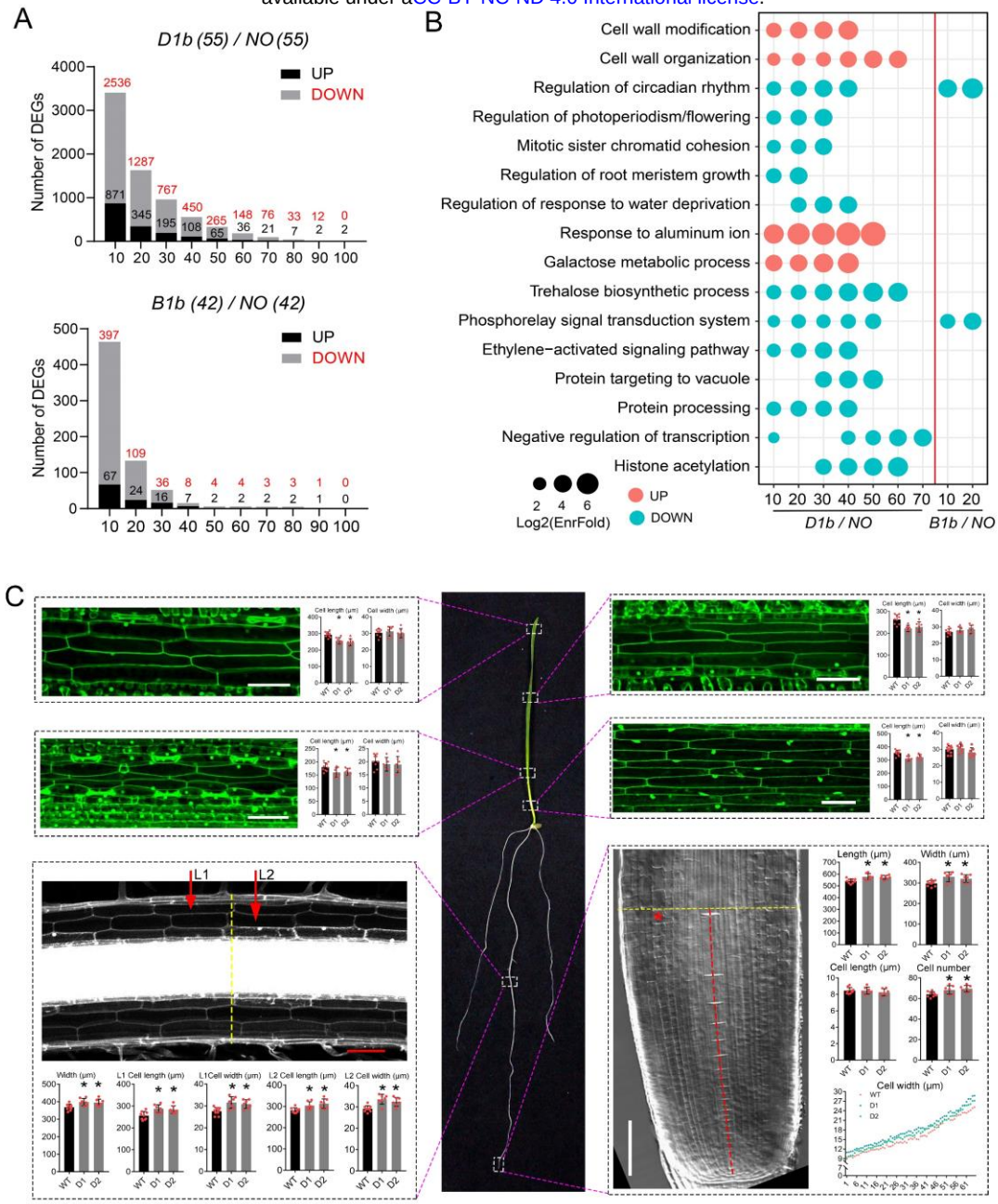

Figure 5. *Rht-D1b* significantly changed the cell size of roots.

(A) The numbers of DEGs in the comparisons between *D1b* and *NO* genotypes and *B1b* and *NO* genotypes. The X-axis represents the observation numbers of DEGs in the 100 permutations. The numbers in brackets indicate 60% of the accessions contained in the smaller compared group, and these accessions were randomly sampled from each of the two compared groups in the permutation test. NO: *Rht-B1aRht-D1a*; B1b: *Rht-B1bRht-D1a*; D1b*: Rht-B1aRht-D1b*.

(B) GO enrichment analyses of the DEGs in (A). The X-axis represents the observation numbers of DEGs in the 100 permutations. *NO*: *Rht-B1aRht-D1a*; *B1b*: *Rht-B1bRht-D1a*; *D1b: Rht-B1aRht-*

bioRxiv preprint doi: https://doi.org/10.1101/2022.06.02.494553; this version posted June 3, 2022. The copyright holder for this preprint (which was not certified by peer review) is the author/funder, who has granted bioRxiv a license to display the preprint in perpetuity. It is made available under aCC-BY-NC-ND 4.0 International license.

D1b. The full list of enriched terms is included in Supplemental Table S10 and S11.

(C) Confocal laser microscope recorded the cell morphology and size of primary root (meristem and maturation zone) and shoot (leaf and coleoptile) in WT and *pRht-D1*::*Rht-D1*$^{Rht\text{-}D1b}$ transgenic lines (D1/D2). The red dotted line represents meristem length, and the yellow dotted line represents the width of meristem and mature zones. The number, length and width of meristem cells were measured from the cell layer indicated by the asterisk. The cell length and width were calculated using ImageJ software. Bar = 100 μm. * indicates Student's t-test $P < 0.05$.

bioRxiv preprint doi: https://doi.org/10.1101/2022.06.02.494553; this version posted June 3, 2022. The copyright holder for this preprint (which was not certified by peer review) is the author/funder, who has granted bioRxiv a license to display the preprint in perpetuity. It is made available under aCC-BY-NC-ND 4.0 International license.

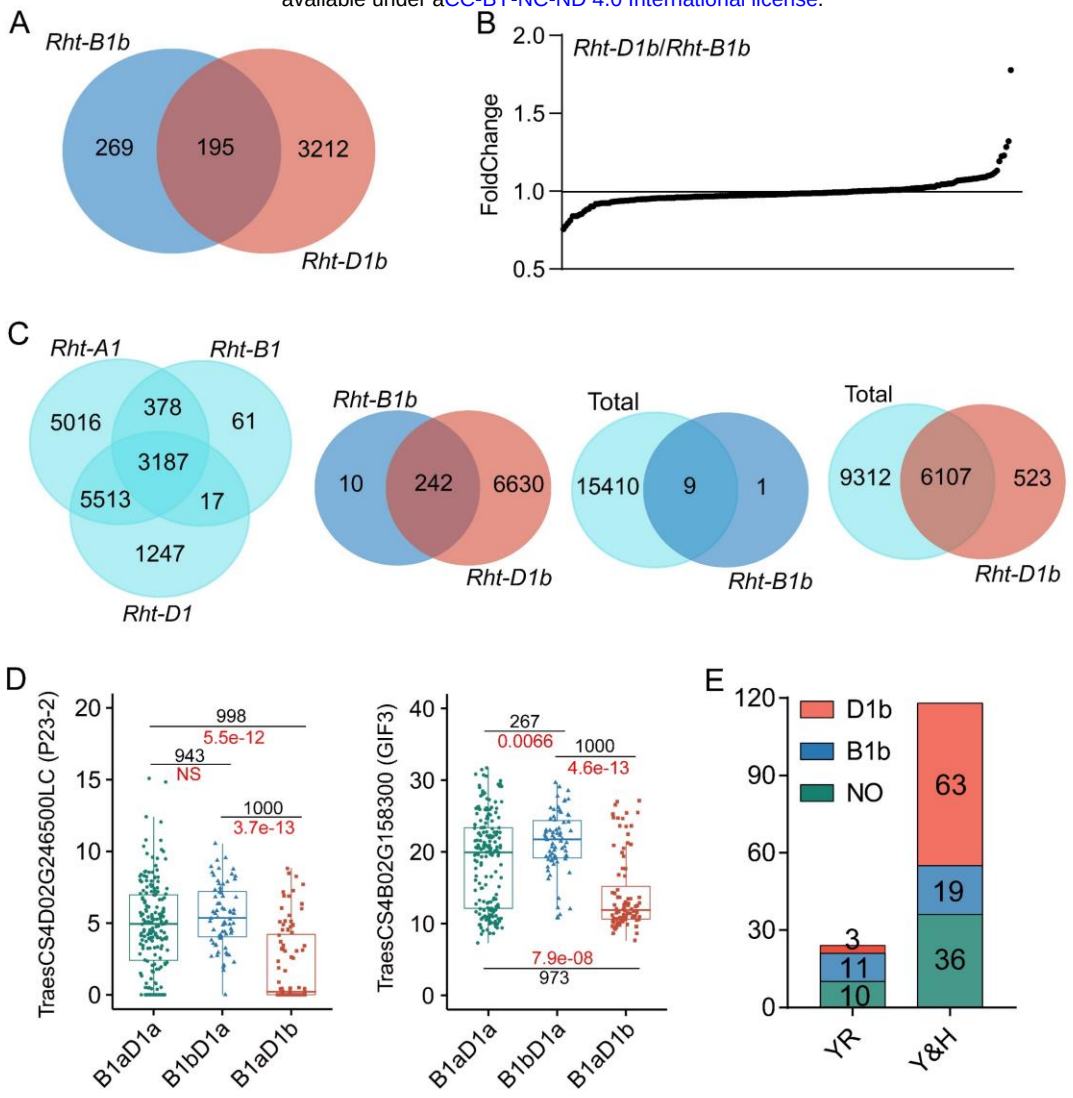

Figure 6. *Rht-D1b* showed a broader regulatory gene spectrum.

(A) Venn diagram of DEGs in *Rht-B1b* vs *NO* genotypes and *Rht-D1b* vs *NO* genotypes. *NO*: *Rht-B1aRht-D1a*.

(B) Fold change (*Rht-D1b*/*Rht-B1b*) of expression levels of the shared DEGs in (A).

(C) The first Venn diagram is the distribution of co-expression genes with *Rht-A1a*, *Rht-B1a* and *Rht-D1a* genes in *NO* genotypes. The second Venn diagram is the distribution of co-expression genes with *Rht-B1* and *Rht-D1* in *Rht-B1b* and *Rht-D1b* genotypes, respectively. The third and fourth Venn diagrams are the distributions of co-expression genes with three *Rhts* in *NO* genotypes ("Total") and the co-expression genes with *Rht-B1* in the *Rht-B1b* genotypes (the third), and the co-expression genes with the *Rht-D1* in the *Rht-D1b* genotypes (the fourth).

(D) Comparisons of expression levels of the wheat homologues of *AtP23-2* and *AtGIF3* between *Rht-B1aRht-D1a* (*B1aD1a*), *Rht-B1bRht-D1a* (*B1bD1a*) and *Rht-B1aRht-D1b* (*B1aD1b*) genotypes.

bioRxiv preprint doi: https://doi.org/10.1101/2022.06.02.494553; this version posted June 3, 2022. The copyright holder for this preprint (which was not certified by peer review) is the author/funder, who has granted bioRxiv a license to display the preprint in perpetuity. It is made available under aCC-BY-NC-ND 4.0 International license.

The red numbers represent *p-values* with Student's t-test using all samples in the two compared groups, and "NS" indicates *P-value* > 0.01. The black numbers indicate the observed number of *P-value* < 0.01 in the 1,000 permutations by randomly sampling 60% of the accessions from each of the two compared groups and further randomly removing accessions from the larger size group to reach the same group size as the smaller one.

(E) Distribution of MC containing *Rht-B1b* and *Rht-D1b* alleles in Yangtze River (YR) and Yellow and Huai (Y&H) winter wheat production regions. *NO: Rht-B1aRht-D1a; B1b: Rht-B1bRht-D1a; D1b: Rht-B1aRht-D1b*.

bioRxiv preprint doi: https://doi.org/10.1101/2022.06.02.494553; this version posted June 3, 2022. The copyright holder for this preprint (which was not certified by peer review) is the author/funder, who has granted bioRxiv a license to display the preprint in perpetuity. It is made available under aCC-BY-NC-ND 4.0 International license.

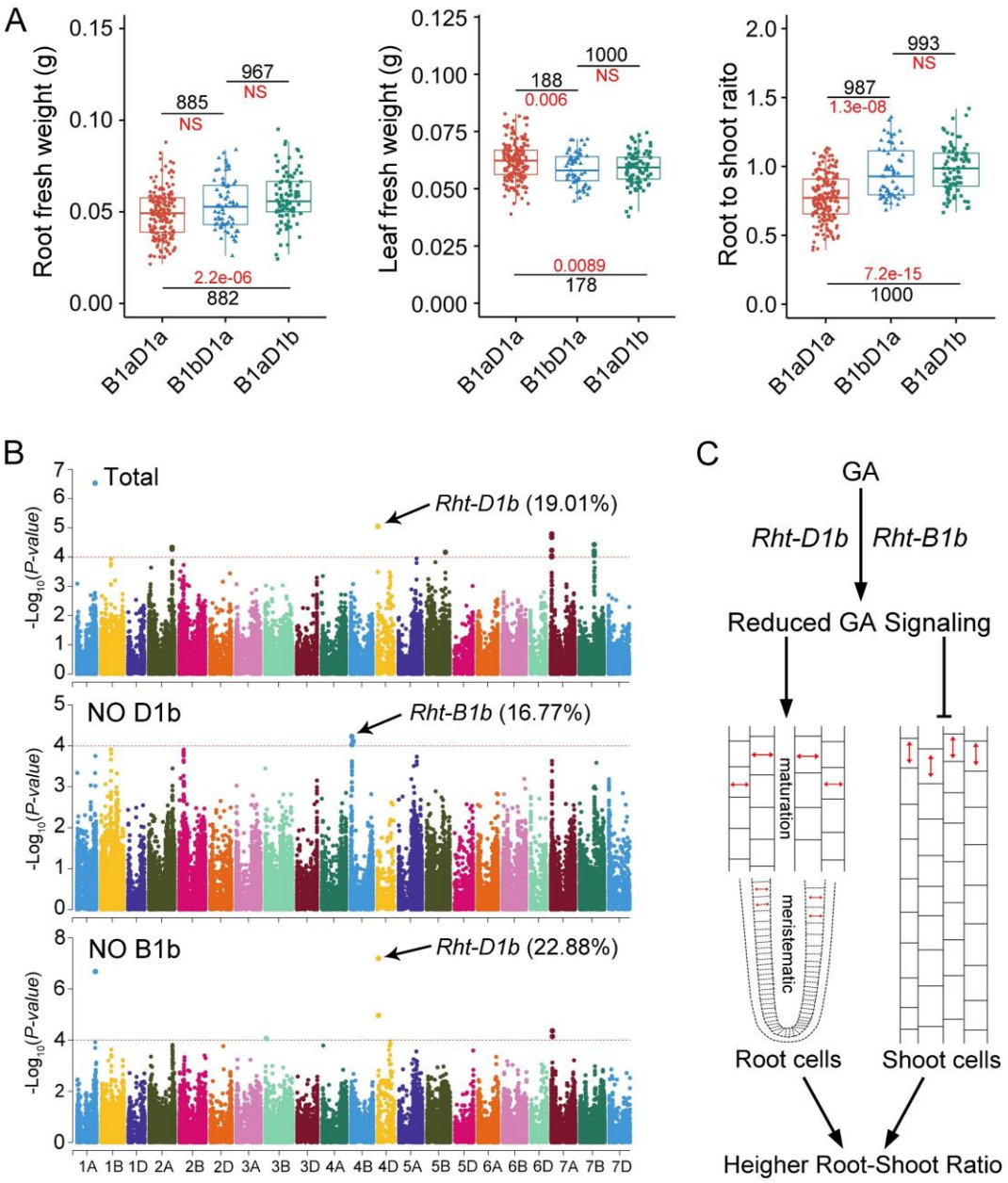

Figure 7. The *Rht-D1b* plays the primary role in increasing the root-shoot ratio in modern wheat cultivars.

(A) Comparison of root fresh weight, leaf fresh weight and root-shoot ratio between *Rht-B1aRht-D1a* (*B1aD1a*), *Rht-B1bRht-D1a* (*B1bD1a*) and *Rht-B1aRht-D1b* (*B1aD1b*) genotypes. The red numbers represent *p-values* with Student's t-test using all samples from the two compared groups, and the "NS" indicates *P-value* > 0.01. The black numbers indicate the observed number of *P-value* < 0.01 in the 1,000 permutations by randomly sampling 60% of the accessions from each of the two compared groups and further randomly removing accessions from the larger size group to reach the

bioRxiv preprint doi: https://doi.org/10.1101/2022.06.02.494553; this version posted June 3, 2022. The copyright holder for this preprint (which was not certified by peer review) is the author/funder, who has granted bioRxiv a license to display the preprint in perpetuity. It is made available under aCC-BY-NC-ND 4.0 International license.

same group size as the smaller one.

(B) Manhattan plots of GWAS analysis of the root-shoot ratio. The upper left letters indicate the genotypes used in the GWAS analysis. From top to bottom, the image shows the GWAS result of total accession and missed accession containing the *Rht-D1b* and *Rht-B1b* genotype. The number represents the phenotypic variances explained by the arrow indicated SNPs.

(C) Model diagram of *Rht-D1b* and *Rht-B1b* regulating wheat seedling development. The introduction of *Rht-D1b* and *Rht-B1b* suppressed the GA signaling, which conferred distinct GA responses between above- and under-ground tissues that increased the cell width in root and inhibited the cell length in above-ground tissue, resulting in a bigger root system and a higher root-shoot ratio.

bioRxiv preprint doi: https://doi.org/10.1101/2022.06.02.494553; this version posted June 3, 2022. The copyright holder for this preprint (which was not certified by peer review) is the author/funder, who has granted bioRxiv a license to display the preprint in perpetuity. It is made available under aCC-BY-NC-ND 4.0 International license.

Parsed Citations

Abbo, S., Pinhasi van-Oss, R., Gopher, A., Saranga, Y., Ofner, I., Peleg, Z. (2014). Plant domestication versus crop evolution: a conceptual framework for cereals and grain legumes. Trends Plant Sci 19, 351-360.
Google Scholar: Author Only Title Only Author and Title

Alexander, D.H., Novembre, J., Lange, K. (2009). Fast model-based estimation of ancestry in unrelated individuals. Genome Res 19, 1655-1664.
Google Scholar: Author Only Title Only Author and Title

Azodi, C.B., Pardo, J., VanBuren, R., de Los Campos, G., Shiu, S.H. (2020). Transcriptome-Based Prediction of Complex Traits in Maize. Plant Cell 32, 139-151.
Google Scholar: Author Only Title Only Author and Title

Bacher, H., Zhu, F., Gao, T., Liu, K., Dhatt, B.K., Awada, T., Zhang, C., Distelfeld, A., Yu, H., Peleg, Z., Walia, H. (2021). Wild emmer introgression alters root-to-shoot growth dynamics in durum wheat in response to water stress. Plant Physiol 187, 1149-1162.
Google Scholar: Author Only Title Only Author and Title

Binenbaum, J., Weinstain, R., Shani, E. (2018). Gibberellin Localization and Transport in Plants. Trends Plant Sci 23, 410-421.
Google Scholar: Author Only Title Only Author and Title

Bolger, A.M., Lohse, M., Usadel, B. (2014). Trimmomatic: a flexible trimmer for Illumina sequence data. Bioinformatics 30, 2114-2120.
Google Scholar: Author Only Title Only Author and Title

Bray, N.L., Pimentel, H., Melsted, P., Pachter, L. (2016). Near-optimal probabilistic RNA-seq quantification. Nat Biotechnol 34, 525-527.
Google Scholar: Author Only Title Only Author and Title

Browning, B.L., Zhou, Y., Browning, S.R. (2018). A One-Penny Imputed Genome from Next-Generation Reference Panels. Am J Hum Genet 103, 338-348.
Google Scholar: Author Only Title Only Author and Title

Bulik-Sullivan, B., Finucane, H.K., Anttila, V., Gusev, A., Day, F.R., Loh, P.R., Duncan, L., Perry, J.R., Patterson, N., Robinson, E.B., Daly, M.J., Price, A.L., Neale, B.M. (2015). An atlas of genetic correlations across human diseases and traits. Nat Genet 47, 1236-1241.
Google Scholar: Author Only Title Only Author and Title

Calleja-Cabrera, J., Boter, M., Oñate-Sánchez, L., Pernas, M. (2020). Root Growth Adaptation to Climate Change in Crops. Front Plant Sci 11, 544.
Google Scholar: Author Only Title Only Author and Title

Cantalapiedra, C.P., Hernandez-Plaza, A., Letunic, I., Bork, P., Huerta-Cepas, J. (2021). eggNOG-mapper v2: Functional Annotation, Orthology Assignments, and Domain Prediction at the Metagenomic Scale. Mol Biol Evol 38, 5825-5829.
Google Scholar: Author Only Title Only Author and Title

Chen, J.H., Jiang, H.W., Hsieh, E.J., Chen, H.Y., Chien, C.T., Hsieh, H.L., Lin, T.P. (2012). Drought and salt stress tolerance of an Arabidopsis glutathione S-transferase U17 knockout mutant are attributed to the combined effect of glutathione and abscisic acid. Plant Physiol 158, 340-351.
Google Scholar: Author Only Title Only Author and Title

Chen, W., Wu, Y., Zheng, Z., Qi, T., Visscher, P.M., Zhu, Z., Yang, J. (2021). Improved analyses of GWAS summary statistics by reducing data heterogeneity and errors. Nat Commun 12, 7117.
Google Scholar: Author Only Title Only Author and Title

Cingolani, P., Platts, A., Wang le, L., Coon, M., Nguyen, T., Wang, L., Land, S.J., Lu, X., Ruden, D.M. (2012). A program for annotating and predicting the effects of single nucleotide polymorphisms, SnpEff: SNPs in the genome of Drosophila melanogaster strain w1118; iso-2; iso-3. Fly (Austin) 6, 80-92.
Google Scholar: Author Only Title Only Author and Title

D'Alessandro, S., Golin, S., Hardtke, C.S., Lo Schiavo, F., Zottini, M. (2015). The co-chaperone p23 controls root development through the modulation of auxin distribution in the Arabidopsis root meristem. J Exp Bot 66, 5113-5122.
Google Scholar: Author Only Title Only Author and Title

De Smet, I., Vassileva, V., De Rybel, B., Levesque, M.P., Grunewald, W., Van Damme, D., Van Noorden, G., Naudts, M., Van Isterdael, G., De Clercq, R., Wang, J.Y., Meuli, N., Vanneste, S., Friml, J., Hilson, P., Jürgens, G., Ingram, G.C., Inzé, D., Benfey, P.N., Beeckman, T. (2008). Receptor-like kinase ACR4 restricts formative cell divisions in the Arabidopsis root. Science 322, 594-597.
Google Scholar: Author Only Title Only Author and Title

bioRxiv preprint doi: https://doi.org/10.1101/2022.06.02.494553; this version posted June 3, 2022. The copyright holder for this preprint (which was not certified by peer review) is the author/funder, who has granted bioRxiv a license to display the preprint in perpetuity. It is made available under aCC-BY-NC-ND 4.0 International license.

de Vries, F.T., Griffiths, R.I., Knight, C.G., Nicolitch, O., Williams, A. (2020). Harnessing rhizosphere microbiomes for drought-resilient crop production. Science 368, 270-274.
Google Scholar: Author Only Title Only Author and Title

Den Herder, G., Van Isterdael, G., Beeckman, T., De Smet, I. (2010). The roots of a new green revolution. Trends Plant Sci 15, 600-607.
Google Scholar: Author Only Title Only Author and Title

Dobin, A., Davis, C.A., Schlesinger, F., Drenkow, J., Zaleski, C., Jha, S., Batut, P., Chaisson, M., Gingeras, T.R. (2013). STAR: ultrafast universal RNA-seq aligner. Bioinformatics 29, 15-21.
Google Scholar: Author Only Title Only Author and Title

Fauman, E.B. (2020). Current Techniques for Complex Phenotypes: GWAS of the Electrocardiogram. Trends Genet 36, 897-899.
Google Scholar: Author Only Title Only Author and Title

Fu, J., Cheng, Y., Linghu, J., Yang, X., Kang, L., Zhang, Z., Zhang, J., He, C., Du, X., Peng, Z., Wang, B., Zhai, L., Dai, C., Xu, J., Wang, W., Li, X., Zheng, J., Chen, L., Luo, L., Liu, J., Qian, X., Yan, J., Wang, J., Wang, G. (2013). RNA sequencing reveals the complex regulatory network in the maize kernel. Nat Commun 4, 2832.
Google Scholar: Author Only Title Only Author and Title

Gao, Z., Shi, Z., Zhang, A., Guo, J. (2015). Distribution of genes associated with yield potential and water-saving in Chinese Zone II wheat detected by developed functional markers. Journal of genetics 94, 35-42.
Google Scholar: Author Only Title Only Author and Title

Gilliland, L.U., Pawloski, L.C., Kandasamy, M.K., Meagher, R.B. (2003). Arabidopsis actin gene ACT7 plays an essential role in germination and root growth. The Plant Journal 33, 319-328.
Google Scholar: Author Only Title Only Author and Title

Godfray, H.C., Beddington, J.R., Crute, I.R., Haddad, L., Lawrence, D., Muir, J.F., Pretty, J., Robinson, S., Thomas, S.M., Toulmin, C. (2010). Food security: the challenge of feeding 9 billion people. Science 327, 812-818.
Google Scholar: Author Only Title Only Author and Title

Golan, G., Hendel, E., Méndez Espitia, G.E., Schwartz, N., Peleg, Z. (2018). Activation of seminal root primordia during wheat domestication reveals underlying mechanisms of plant resilience. Plant Cell Environ 41, 755-766.
Google Scholar: Author Only Title Only Author and Title

Guedira, M., Brown-Guedira, G., Van Sanford, D., Sneller, C., Souza, E., Marshall, D. (2010). Distribution of Rht Genes in Modern and Historic Winter Wheat Cultivars from the Eastern and Central USA. Crop Sci 50, 1811-1822.
Google Scholar: Author Only Title Only Author and Title

Hao, C., Jiao, C., Hou, J., Li, T., Liu, H., Wang, Y., Zheng, J., Liu, H., Bi, Z., Xu, F., Zhao, J., Ma, L., Wang, Y., Majeed, U., Liu, X., Appels, R., Maccaferri, M., Tuberosa, R., Lu, H., Zhang, X. (2020). Resequencing of 145 Landmark Cultivars Reveals Asymmetric Sub-genome Selection and Strong Founder Genotype Effects on Wheat Breeding in China. Mol Plant 13, 1733-1751.
Google Scholar: Author Only Title Only Author and Title

Hayta, S., Smedley, M.A., Demir, S.U., Blundell, R., Hinchliffe, A., Atkinson, N., Harwood, W.A. (2019). An efficient and reproducible Agrobacterium-mediated transformation method for hexaploid wheat (Triticum aestivum L.). Plant Methods 15, 121.
Google Scholar: Author Only Title Only Author and Title

Hendel, E., Bacher, H., Oksenberg, A., Walia, H., Schwartz, N., Peleg, Z. (2021). Deciphering the genetic basis of wheat seminal root anatomy uncovers ancestral axial conductance alleles. Plant Cell Environ 44, 1921-1934.
Google Scholar: Author Only Title Only Author and Title

Hou, L., Zhang, A., Wang, R., Zhao, P., Zhang, D., Jiang, Y., Diddugodage, C.J., Wang, X., Ni, Z., Xu, S. (2019). Brassinosteroid Regulates Root Development with Highly Redundant Genes in Hexaploid Wheat. Plant Cell Physiol 60, 1761-1777.
Google Scholar: Author Only Title Only Author and Title

Hu, Y., Chen, J., Fang, L., Zhang, Z., Ma, W., Niu, Y., Ju, L., Deng, J., Zhao, T., Lian, J., Baruch, K., Fang, D., Liu, X., Ruan, Y.L., Rahman, M.U., Han, J., Wang, K., Wang, Q., Wu, H., Mei, G., Zang, Y., Han, Z., Xu, C., Shen, W., Yang, D., Si, Z., Dai, F., Zou, L., Huang, F., Bai, Y., Zhang, Y., Brodt, A., Ben-Hamo, H., Zhu, X., Zhou, B., Guan, X., Zhu, S., Chen, X., Zhang, T. (2019). Gossypium barbadense and Gossypium hirsutum genomes provide insights into the origin and evolution of allotetraploid cotton. Nat Genet 51, 739-748.
Google Scholar: Author Only Title Only Author and Title

International Wheat Genome Sequencing Consortium (IWGSC) (2018). Shifting the limits in wheat research and breeding using a fully annotated reference genome. Science 361, 6403.
Google Scholar: Author Only Title Only Author and Title

Khan, M.A., Gemenet, D.C., Villordon, A. (2016). Root System Architecture and Abiotic Stress Tolerance: Current Knowledge in Root and Tuber Crops. Front Plant Sci 7, 1584.

bioRxiv preprint doi: https://doi.org/10.1101/2022.06.02.494553; this version posted June 3, 2022. The copyright holder for this preprint (which was not certified by peer review) is the author/funder, who has granted bioRxiv a license to display the preprint in perpetuity. It is made available under aCC-BY-NC-ND 4.0 International license.

Google Scholar: Author Only Title Only Author and Title

Kremling, K.A.G., Diepenbrock, C.H., Gore, M.A., Buckler, E.S., Bandillo, N.B. (2019). Transcriptome-Wide Association Supplements Genome-Wide Association in Zea mays. G3 (Bethesda) 9, 3023-3033.
Google Scholar: Author Only Title Only Author and Title

Lanning, S.P., Martin, J.M., Stougaard, R.N., Guillen-Portal, F.R., Talbert, L.E. (2012). Evaluation of Near-Isogenic Lines for Three Height-Reducing Genes in Hard Red Spring Wheat. Crop Sci 52, 1145-1152.
Google Scholar: Author Only Title Only Author and Title

Lee, B.H., Ko, J.H., Lee, S., Lee, Y., Pak, J.H., Kim, J.H. (2009). The Arabidopsis GRF-INTERACTING FACTOR gene family performs an overlapping function in determining organ size as well as multiple developmental properties. Plant Physiol 151, 655-668.
Google Scholar: Author Only Title Only Author and Title

Letunic, I., Bork, P. (2021). Interactive Tree Of Life (iTOL) v5: an online tool for phylogenetic tree display and annotation. Nucleic Acids Res 49, W293-2296.
Google Scholar: Author Only Title Only Author and Title

Li, H., Durbin, R. (2010). Fast and accurate long-read alignment with Burrows-Wheeler transform. Bioinformatics 26, 589-595.
Google Scholar: Author Only Title Only Author and Title

Li, Y., Ge, X., Peng, F., Li, W., Li, J.J. (2022). Exaggerated false positives by popular differential expression methods when analyzing human population samples. Genome Biol 23, 79.
Google Scholar: Author Only Title Only Author and Title

Liu, Q., Wu, K., Harberd, N.P., Fu, X. (2021). Green Revolution DELLAs: From translational reinitiation to future sustainable agriculture. Mol Plant 14, 547-549.
Google Scholar: Author Only Title Only Author and Title

Lynch, J. (1995). Root Architecture and Plant Productivity. Plant Physiol 109, 7-13.
Google Scholar: Author Only Title Only Author and Title

Lynch, J.P. (2007). Roots of the Second Green Revolution. Australian Journal of Botany 55, 493-512.
Google Scholar: Author Only Title Only Author and Title

McKenna, A., Hanna, M., Banks, E., Sivachenko, A., Cibulskis, K., Kernytsky, A., Garimella, K., Altshuler, D., Gabriel, S., Daly, M., DePristo, M.A. (2010). The Genome Analysis Toolkit: a MapReduce framework for analyzing next-generation DNA sequencing data. Genome Res 20, 1297-1303.
Google Scholar: Author Only Title Only Author and Title

Ohashi-Ito, K., Fukuda, H. (2003). HD-zip III homeobox genes that include a novel member, ZeHB-13 (Zinnia)/ATHB-15 (Arabidopsis), are involved in procambium and xylem cell differentiation. Plant Cell Physiol 44, 1350-1358.
Google Scholar: Author Only Title Only Author and Title

Pearce, S., Saville, R., Vaughan, S.P., Chandler, P.M., Wilhelm, E.P., Sparks, C.A., Al-Kaff, N., Korolev, A., Boulton, M.I., Phillips, A.L., Hedden, P., Nicholson, P., Thomas, S.G. (2011). Molecular characterization of Rht-1 dwarfing genes in hexaploid wheat. Plant Physiol 157, 1820-1831.
Google Scholar: Author Only Title Only Author and Title

Qin, H., Pandey, B.K., Li, Y., Huang, G., Wang, J., Quan, R., Zhou, J., Zhou, Y., Miao, Y., Zhang, D., Bennett, M.J., Huang, R. (2022). Orchestration of ethylene and gibberellin signals determines primary root elongation in rice. Plant Cell 34, 1273-1288.
Google Scholar: Author Only Title Only Author and Title

Ramirez-Gonzalez, R.H., Borrill, P., Lang, D., Harrington, S.A., Brinton, J., Venturini, L., Davey, M., Jacobs, J., van Ex, F., Pasha, A., Khedikar, Y., Robinson, S.J., Cory, A.T., Florio, T., Concia, L., Juery, C., Schoonbeek, H., Steuernagel, B., Xiang, D., Ridout, C.J., Chalhoub, B., Mayer, K.F.X., Benhamed, M., Latrasse, D., Bendahmane, A., International Wheat Genome Sequencing, C., Wulff, B.B.H., Appels, R., Tiwari, V., Datla, R., Choulet, F., Pozniak, C.J., Provart, N.J., Sharpe, A.G., Paux, E., Spannagl, M., Brautigam, A., Uauy, C. (2018). The transcriptional landscape of polyploid wheat. Science 361, 6403.
Google Scholar: Author Only Title Only Author and Title

Rizza, A., Jones, A.M. (2019). The makings of a gradient: spatiotemporal distribution of gibberellins in plant development. Curr Opin Plant Biol 47, 9-15.
Google Scholar: Author Only Title Only Author and Title

Shani, E., Weinstain, R., Zhang, Y., Castillejo, C., Kaiserli, E., Chory, J., Tsien, R.Y., Estelle, M. (2013). Gibberellins accumulate in the elongating endodermal cells of Arabidopsis root. Proc Natl Acad Sci U S A 110, 4834-4839.
Google Scholar: Author Only Title Only Author and Title

Sherman, J.D., Nash, D., Lanning, S.P., Martin, J.M., Blake, N.K., Morris, C.F., Talbert, L.E. (2014). Genetics of End-Use Quality Differences between a Modern and Historical Spring Wheat. Crop Sci 54, 1972-1980.

bioRxiv preprint doi: https://doi.org/10.1101/2022.06.02.494553; this version posted June 3, 2022. The copyright holder for this preprint (which was not certified by peer review) is the author/funder, who has granted bioRxiv a license to display the preprint in perpetuity. It is made available under aCC-BY-NC-ND 4.0 International license.

Google Scholar: Author Only Title Only Author and Title

Snowdon, R.J., Wittkop, B., Chen, T.W., Stahl, A. (2020). Crop adaptation to climate change as a consequence of long-term breeding. Theor Appl Genet 134, 1613-1623.
Google Scholar: Author Only Title Only Author and Title

Soneson, C., Love, M.I., Robinson, M.D. (2015). Differential analyses for RNA-seq: transcript-level estimates improve gene-level inferences. F1000Res 4, 1521.
Google Scholar: Author Only Title Only Author and Title

Stamatakis, A. (2014). RAxML version 8: a tool for phylogenetic analysis and post-analysis of large phylogenies. Bioinformatics 30, 1312-1313.
Google Scholar: Author Only Title Only Author and Title

Tang, S., Zhao, H., Lu, S., Yu, L., Zhang, G., Zhang, Y., Yang, Q.Y., Zhou, Y., Wang, X., Ma, W., Xie, W., Guo, L. (2021). Genome- and transcriptome-wide association studies provide insights into the genetic basis of natural variation of seed oil content in Brassica napus. Mol Plant 14, 470-487.
Google Scholar: Author Only Title Only Author and Title

Tanimoto, E. (2012). Tall or short? Slender or thick? A plant strategy for regulating elongation growth of roots by low concentrations of gibberellin. Ann Bot 110, 373-381.
Google Scholar: Author Only Title Only Author and Title

Teotia, S., Lamb, R.S. (2011). RCD1 and SRO1 are necessary to maintain meristematic fate in Arabidopsis thaliana. J Exp Bot 62, 1271-1284.
Google Scholar: Author Only Title Only Author and Title

Topham, A.T., Taylor, R.E., Yan, D., Nambara, E., Johnston, I.G., Bassel, G.W. (2017). Temperature variability is integrated by a spatially embedded decision-making center to break dormancy in Arabidopsis seeds. Proc Natl Acad Sci U S A 114, 6629-6634.
Google Scholar: Author Only Title Only Author and Title

Truernit, E., Siemering, K.R., Hodge, S., Grbic, V., Haseloff, J. (2006). A map of KNAT gene expression in the Arabidopsis root. Plant Mol Biol 60, 1-20.
Google Scholar: Author Only Title Only Author and Title

Van De Velde, K., Thomas, S.G., Heyse, F., Kaspar, R., Van Der Straeten, D., Rohde, A. (2021). N-terminal truncated RHT-1 proteins generated by translational reinitiation cause semi-dwarfing of wheat Green Revolution alleles. Mol Plant 14, 679-687.
Google Scholar: Author Only Title Only Author and Title

van de Wouw, M., van Hintum, T., Kik, C., van Treuren, R., Visser, B. (2010). Genetic diversity trends in twentieth century crop cultivars: a meta analysis. Theor Appl Genet 120, 1241-1252.
Google Scholar: Author Only Title Only Author and Title

van der Bom, F.J.T., Williams, A., Bell, M.J. (2020). Root architecture for improved resource capture: trade-offs in complex environments. J Exp Bot 71, 5752-5763.
Google Scholar: Author Only Title Only Author and Title

Wainberg, M., Sinnott-Armstrong, N., Mancuso, N., Barbeira, A.N., Knowles, D.A., Golan, D., Ermel, R., Ruusalepp, A., Quertermous, T., Hao, K., Björkegren, J.L.M., Im, H.K., Pasaniuc, B., Rivas, M.A., Kundaje, A. (2019). Opportunities and challenges for transcriptome-wide association studies. Nat Genet 51, 592-599.
Google Scholar: Author Only Title Only Author and Title

Wang, J., Zhang, Z. (2021). GAPIT Version 3: Boosting Power and Accuracy for Genomic Association and Prediction. Genomics Proteomics Bioinformatics 19, 629-640.
Google Scholar: Author Only Title Only Author and Title

Watt, M., Magee, L.J., McCully, M.E. (2008). Types, structure and potential for axial water flow in the deepest roots of field-grown cereals. New Phytol 178, 135-146.
Google Scholar: Author Only Title Only Author and Title

Wu, J., Kong, X., Wan, J., Liu, X., Zhang, X., Guo, X., Zhou, R., Zhao, G., Jing, R., Fu, X., Jia, J. (2011). Dominant and pleiotropic effects of a GAI gene in wheat results from a lack of interaction between DELLA and GID1. Plant Physiol 157, 2120-2130.
Google Scholar: Author Only Title Only Author and Title

Wu, Y., Chang, Y., Luo, L., Tian, W., Gong, Q., Liu, X. (2022). Abscisic acid employs NRP-dependent PIN2 vacuolar degradation to suppress auxin-mediated primary root elongation in Arabidopsis. New Phytol 233, 297-312.
Google Scholar: Author Only Title Only Author and Title

Wu, Y., Thorne, E.T., Sharp, R.E., Cosgrove, D.J. (2001). Modification of expansin transcript levels in the maize primary root at low water potentials. Plant Physiol 126, 1471-1479.
Google Scholar: Author Only Title Only Author and Title

bioRxiv preprint doi: https://doi.org/10.1101/2022.06.02.494553; this version posted June 3, 2022. The copyright holder for this preprint (which was not certified by peer review) is the author/funder, who has granted bioRxiv a license to display the preprint in perpetuity. It is made available under aCC-BY-NC-ND 4.0 International license.

Wurschum, T., Langer, S.M., Longin, C.F. (2015). Genetic control of plant height in European winter wheat cultivars. TAG. Theoretical and applied genetics. Theor Appl Genet 128, 865-874.
Google Scholar: Author Only Title Only Author and Title

Wurschum, T., Langer, S.M., Longin, C.F.H., Tucker, M.R., and Leiser, W.L. (2017). A modern Green Revolution gene for reduced height in wheat. Plant J 92, 892-903.
Google Scholar: Author Only Title Only Author and Title

Wurschum, T., Liu, G., Boeven, P.H.G., Longin, C.F.H., Mirdita, V., Kazman, E., Zhao, Y., Reif, J.C. (2018). Exploiting the Rht portfolio for hybrid wheat breeding. Theor Appl Genet 131, 1433-1442.
Google Scholar: Author Only Title Only Author and Title

Yokoyama, A., Yamashino, T., Amano, Y., Tajima, Y., Imamura, A., Sakakibara, H., Mizuno, T. (2007). Type-B ARR transcription factors, ARR10 and ARR12, are implicated in cytokinin-mediated regulation of protoxylem differentiation in roots of Arabidopsis thaliana. Plant Cell Physiol 48, 84-96.
Google Scholar: Author Only Title Only Author and Title

Yu, G., Wang, L.G., Han, Y., He, Q.Y. (2012). clusterProfiler: an R package for comparing biological themes among gene clusters. OMICS 16, 284-287.
Google Scholar: Author Only Title Only Author and Title

Yue, K., Sandal, P., Williams, E.L., Murphy, E., Stes, E., Nikonorova, N., Ramakrishna, P., Czyzewicz, N., Montero-Morales, L., Kumpf, R., Lin, Z., van de Cotte, B., Iqbal, M., Van Bel, M., Van De Slijke, E., Meyer, M.R., Gadeyne, A., Zipfel, C., De Jaeger, G., Van Montagu, M., Van Damme, D., Gevaert, K., Rao, A.G., Beeckman, T., De Smet, I. (2016). PP2A-3 interacts with ACR4 and regulates formative cell division in the Arabidopsis root. Proc Natl Acad Sci U S A 113, 1447-1452.
Google Scholar: Author Only Title Only Author and Title

Zhang, L., Su, W., Tao, R., Zhang, W., Chen, J., Wu, P., Yan, C., Jia, Y., Larkin, R.M., Lavelle, D., Truco, M.J., Chin-Wo, S.R., Michelmore, R.W., Kuang, H. (2017). RNA sequencing provides insights into the evolution of lettuce and the regulation of flavonoid biosynthesis. Nat Commun 8, 2264.
Google Scholar: Author Only Title Only Author and Title

Zhang, X., Yang, S., Zhou, Y., He, Z., Xia, X. (2006). Distribution of the Rht-B1b, Rht-D1b and Rht8 reduced height genes in autumn-sown Chinese wheats detected by molecular markers. Euphytica 152, 109-116.
Google Scholar: Author Only Title Only Author and Title

Zhou, Y., Zhao, X., Li, Y., Xu, J., Bi, A., Kang, L., Xu, D., Chen, H., Wang, Y., Wang, Y.G., Liu, S., Jiao, C., Lu, H., Wang, J., Yin, C., Jiao, Y., Lu, F. (2020). Triticum population sequencing provides insights into wheat adaptation. Nat Genet 52, 1412-1422.
Google Scholar: Author Only Title Only Author and Title

Zubo, Y.O., Blakley, I.C., Yamburenko, M.V., Worthen, J.M., Street, I.H., Franco-Zorrilla, J.M., Zhang, W., Hill, K., Raines, T., Solano, R., Kieber, J.J., Loraine, A.E., Schaller, G.E. (2017). Cytokinin induces genome-wide binding of the type-B response regulator ARR10 to regulate growth and development in Arabidopsis. Proc Natl Acad Sci U S A 114, E5995-E6004.
Google Scholar: Author Only Title Only Author and Title